DEUTSCHES ELEKTRONEN-SYNCHROTRON DESY

DESY 79/20
April 1979

QUARKONIA

by

M. Krammer and H. Krasemann

NOTKESTRASSE 85 · 2 HAMBURG 52

To be sure that your preprints are promptly included in the
HIGH ENERGY PHYSICS INDEX ,
send them to the following address (if possible by air mail) :

DESY
Bibliothek
Notkestrasse 85
2 Hamburg 52
Germany

Q U A R K O N I A

by

M. Krammer and H. Krasemann

Deutsches Elektronen-Synchrotron DESY, Hamburg

Lectures presented by M. Krammer at the XVIII. Internationale Universitätswochen für Kernphysik, Schladming, Austria, February 28 - March 10, 1979.

Table of Content

1. Introduction

When the J/Ψ and Ψ' were discovered in fall 1974 [1] we all witnessed a dramatic and beautiful revival of the quark model [2]. The predicted new quark flavour, c = charm [3] could be added to the hadron spectroscopy by the interpretation of the new particles as $c\bar{c}$ bound states. It was argued that the new system is nonrelativistic: Charmonium [4]. Whereas the old mesons suffered from the fact that the quarks are extremely relativistic (mass differences are of the order of the masses themselves), in Charmonium the heavy ($\approx$ 1.5 GeV) c-quarks should move relatively slowly, $\beta^2 = (v/c)^2 \approx 0.2$. The well known powerful methods of exploring a nonrelativistic system could be used. This was the source of real excitement about the new particles.

In spring 1977 a still heavier meson family, the $\Upsilon, \Upsilon', \Upsilon''$ [5] was discovered. From the measurement of their leptonic decay widths in DORIS [6] we learned that the charge of the fifth quark [7] is $|e_Q| = 1/3$: we found the bottom quark. The $b\bar{b}$ system, which is supposed to be even much more nonrelativistic than $c\bar{c}$, is thus called Bottonium. We hope to discover a heavier sixth quark flavour, t = top maybe, in the new machines PETRA and PEP. In these lectures we will describe the dynamics of a nonrelativistic $Q\bar{Q}$ bound system, Q = c,b,t,..., called QUARKONIUM.

Quantumchromodynamics [8], QCD, turned out to be the most promising candidate for the theory of quark dynamics, i.e. the strong interactions. QCD is a nonabelian gauge field theory of the interactions of quarks and eight massless vector gauge bosons, the gluons. The coupling constant α_s, renormalized at the relevant momentum transfer q^2 or the corresponding distance R, is a monotonously falling function of $|q^2|$. It tends logarithmically to zero as $|q^2| \to \infty$ or $R \to 0$

$$\alpha_s(q^2) = \frac{12\pi}{33-2N} \cdot \frac{1}{\log(q^2/q_0^2)} + O(\log^{-2}) \qquad (1.1)$$

N = number of light quark flavours

this is called "asymptotic freedom" [9].

If α_s becomes small, perturbation theory is fine and in Born approximation

the quark interaction is just one gluon exchange. The nonabelian selfinteraction of the colour-charged gluons plays no rôle in lowest order graphs, thus QCD is very similar to QED, the static potential for short distances being essentially of the Coulomb type.

α_s becomes large for some large R of the order of 1/2 fm, which is the typical hadron radius. At present this region, where perturbation theory does not work, is subject to educated speculations only [10]: we believe that the rising coupling "confines" the quarks. Models which give a hint at this are lattice gauge theories or the string model.

When QCD is in fact the underlying theory for Quarkonia, we should be able to probe QCD features by studying these systems. First we should be able to probe the one gluon exchange at short distances. The static Coulomb-like potential gives rise to the spin-spin, spin-orbit and tensor interactions known from Positronium, since the quark gluon vertex has the same Dirac structure as the electron photon vertex (γ_μ-coupling). Second, at large distances the "confining" potential should be linear, $V_C(R) = aR$. It should be flavour independent and the interquark force a at large distances should also be somehow related to the inverse Regge slope of the low mass mesons. The "confining" potential should be essentially spin independent [10].

We have no guess for the potential at intermediate distances. In Charmonium a superposition of the spin dependent one gluon exchange potential and the scalar linear potential has worked out rather well [11]. However, this potential is not universal, as we have learned from Bottonium. The intermediate region of the potential has to be treated in a more sophisticated manner.

Besides the spectra, the fine and hyperfine structure we will discuss radiative transitions in some detail. Chapter 7 will be devoted to the puzzling states X(2.83), χ(3.45) and χ(3.59/3.18).

As an application of QCD we will describe the gluonic annihilation of Quarkonia, which leads to the total hadronic decay width via a nonperturbative dressing mechanism. With the experimentally accessible regime of

c.m. energies of 10 GeV or more, the gluons which govern annihilations in QCD, might show up as hadron jets [12]. These jets should carry the directed momentum of the initial gluon. In angular distributions of these jets one should be able to measure gluon helicities [12,13]. One can further speculate on the existence of glueballs [14] in Quarkonium decays. It is rather difficult, however, to find an easy test of the nonabelian gluon self coupling. Nevertheless, finding the gluons is very important: they are the gauge bosons of QCD and a proof of their existence is as crucial for QCD as a proof of the existence of Z^0 and $W^{\pm}$ for the Salam-Weinberg theory.

2. The Spectra

Quarkonium is essentially nonrelativistic. The perturbative Hamiltonian is then obtained from the Bethe Salpeter equation in nonrelativistic approximation or from the exact relativistic scattering amplitude (Born graph only). One obtains the Schrödinger equation in zeroth order of β^2 and the Fermi-Breit Hamiltonian terms up to order β^2. In o^{th} order

$$H^o = 2 m_Q + \vec{p}^{\,2}/m_Q + V(R) + \text{const.} \tag{2.1}$$

a) Charmonium

For Charmonium the standard potential used is [11]

$$V(R) = V_{AF}(R) + V_C(R) = -\frac{4}{3}\cdot\frac{\alpha_s}{R} + a\cdot R \tag{2.2}$$

V_{AF} is the "asymptotically free" short distance part due to one gluon exchange. -4/3 is a group factor from $SU(3)_{colour}$ and α_s is the effective coupling. For this one can take two points of view. Either α_s is R-dependent [15] or α_s is a constant, different for each quark flavour mass: [9]

$$\alpha_s(M_2^2) = \alpha_s(M_1^2)\left[1 - \frac{33-2N}{12\pi}\alpha_s(M_1^2)\log(M_1^2/M_2^2)\right]^{-1} \tag{2.3}$$

N = number of "light" quarks

In the standard calculations [11,16] the second point of view is taken.

At large distances the potential should be "confining". The linear potential is suggested by lattice gauge theories, or string models where the field lines are parallel and the force between two coloured constituents is constant:

One example is the Meissner effect in superconductors of the second kind and another example is QED in one space dimension.

The potential and the structure of the spectrum is shown in Fig. 2.1 and is compared with the experimental Charmonium.

The parameters are determined as

$$a = 1 - 0.9\ \mathrm{GeV/fm} \quad \text{from } \psi' - J/\psi$$

$$\alpha_s = 0.3 - 0.4 \quad \text{from} \quad \frac{|\psi_{\psi'}(0)|^2}{|\psi_{J/\psi}(0)|^2} = \frac{M_{\psi'}^2 \Gamma_{e\bar{e}}(\psi')}{M_{J/\psi}^2 \Gamma_{e\bar{e}}(J/\psi)} = \frac{(3.7\ \mathrm{GeV})^2\, 2.2\ \mathrm{keV}}{(3.1\ \mathrm{GeV})^2\, 4.8\ \mathrm{keV}} \tag{2.4}$$

or from the center of gravity of the P waves. The quark mass only slightly influences this fit. It mainly influences the wave functions themselves, the dipole matrix elements and the velocity of the quarks. For the dipole matrix elements one would like a large quark mass, $m_c \simeq 2$ GeV. Fitting m_c to $|\psi(0)|^2$ from the naive [+] Van-Royen-Weisskopf formula [17]

$$\Gamma_{e\bar{e}}(V) = 16\pi\alpha^2 e_Q^2 \frac{|\psi_V(0)|^2}{M_V^2} = \alpha^2 e_Q^2 \frac{|R_V(0)|^2}{(M_V/2)^2} \tag{2.5}$$

gives a rather small value, $m_c \simeq 1.1$ GeV. However, this does not destroy the nonrelativistic approximation. We found $\beta^2 = (v/c)^2 < 0.3$ in J/ψ and $\beta^2 < 0.4$ in ψ' for $m_c = 1.16$ GeV and $\alpha_s < 0.41$. Thus the quark masses are an open question here.

Is the large value of α_s reasonable? From the decay formulae to be described in Chapter 8 one finds α_s(annihilation at 3 GeV) $\simeq 0.2$. However,

---

[+] There is a next order QCD correction to the Schrödinger wave function at the origin $|\psi(0)|^2 \to |\psi(0)|^2\left(1 - \frac{16\alpha_s}{3\pi}\right)$ due to a transverse gluon vertex correction [18]. This is large in Charmonium.

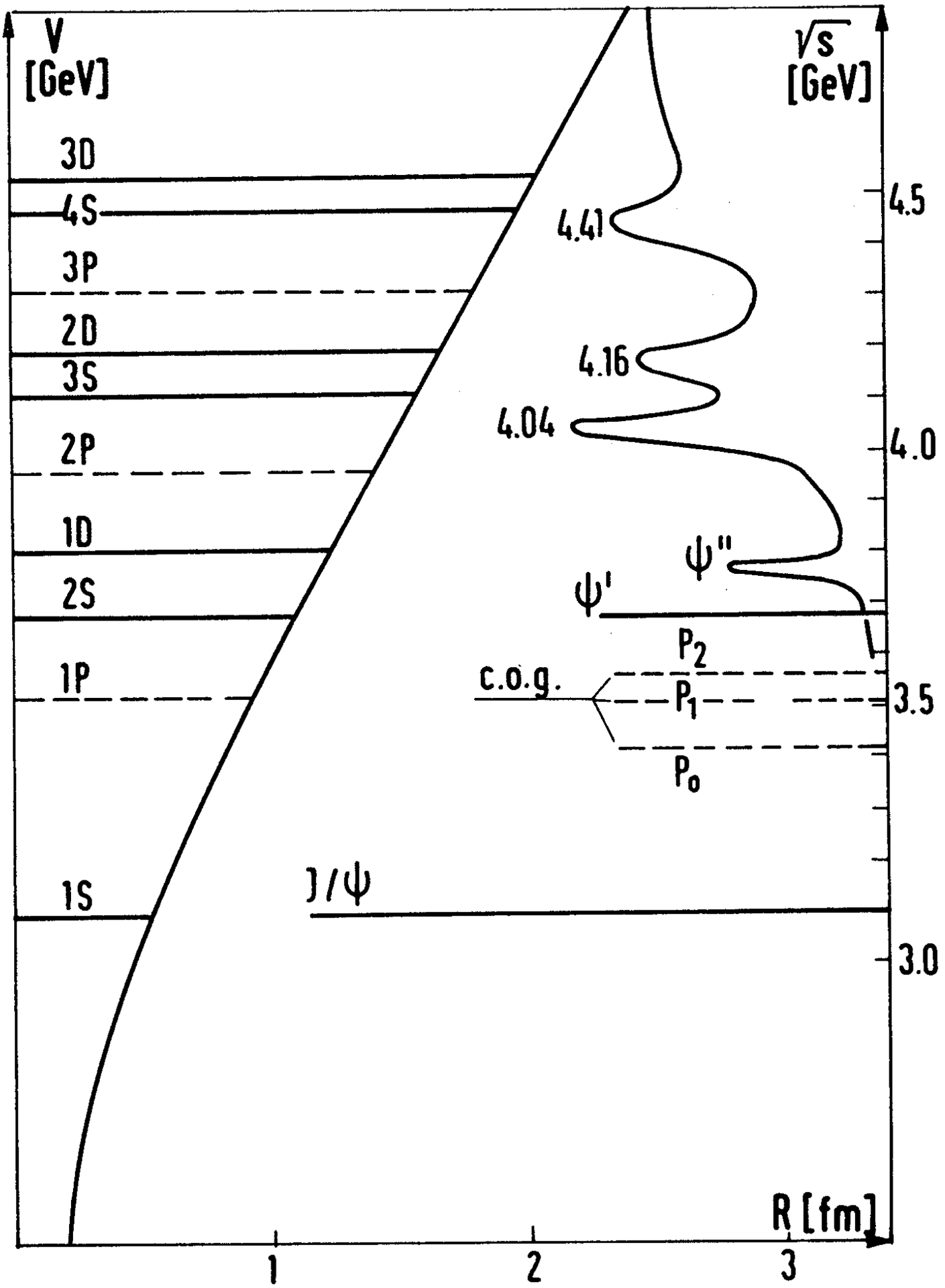

Fig. 2.1. The shape of the standard Charmonium potential (2.2) with $\alpha_s = 0.41$, the spectrum and the experimentally observed Charmonium states. The other parameters are a = 0.8665 GeV/fm and m_c = 1.6 GeV.

this refers to annihilation distances which are shorter than the average interquark distances. Furthermore the probability for three gluons $\longrightarrow$ hadrons may be smaller than one. Then α_s(annihilation) is larger than 0.2. From deep inelastic lepton scattering on the other hand we find $\alpha_s(3\ \text{GeV}) \simeq \alpha_s(0.07\ \text{fm}) \simeq 0.4$ taking the scale parameter $\lambda = 0.5$ GeV. From Fig. 2.1 we see that 0.07 fm is just in the middle of the range where V_{AF} dominates.

It is remarkable to see that the predicted D wave coincides with $\Psi''(3.77)$, especially if the spin-orbit and tensor force splittings are taken into account! Amusingly also the higher S and D waves seem to coincide with the observed peaks in R above 4 GeV. Historical discrepancies in this respect are due to the choice of α_s.

The level sequence in Charmonium is 1S, 1P, 2S, 1D,.. There are two theorems [19] about this ordering, let us quote them here:

i) For $V(R) = \frac{-g^2}{R} + V_c(R)$, where V_c is a confining potential non-singular at the origin, 2S is above 1P if V_c satisfies the following sufficient condition

$$\left(\frac{d}{dR}\right)^2 \left[R\left(2V_c(R) + R\,\frac{dV_c(R)}{dR}\right)\right] > 0 \quad \forall R \qquad \left[V_c(R) = R^{\varepsilon},\ \varepsilon > 0\right] \tag{2.6}$$

ii) $V(R) = \frac{-g^2}{R} + V_c(R)$, where V_c is a non-singular confining potential. If $(d/dR)^3 (R^2 V_c(R))$ is positive, then the 1D state lies above the 2S state, provided

$$\frac{d}{dR}\,\frac{1}{R}\,\frac{d}{dR}\left(2V_c(R) + R\,\frac{dV_c(R)}{dR}\right) < 0 \quad \forall R \qquad \left[V_c(R) = R^{\varepsilon},\ 0 < \varepsilon < 2\right] \tag{2.7}$$

b) Scaling the Schrödinger Equation

We now ask the question whether or not $V_c(R) = aR$ is unique for the next quark flavour (quark mass) as QCD suggests. For this purpose we first consider the scaling behaviour of the Schrödinger equation. The radial equation

$$\left[\frac{-d^2}{dR^2} + \frac{\ell(\ell+1)}{R^2} + 2\mu\left(V(R) - E\right)\right] u(R) = 0 \quad \text{with } V(R) = a\cdot R^{\varepsilon},\ \varepsilon > -2 \tag{2.8}$$

can be brought into dimensionless form

$$\left[\frac{-d^2}{d\varrho^2} + \frac{\ell(\ell+1)}{\varrho^2} + \varrho^{\varepsilon} - \xi\right] v(\varrho) = 0 \tag{2.9}$$

with

$$\varrho = R(2\mu a)^{1/(2+\varepsilon)} \quad , \qquad \xi = 2\mu E (2\mu a)^{-2/(2+\varepsilon)} \tag{2.10}$$

From (2.10) one reads off the scaling laws

$$R \sim m^{-1/(2+\varepsilon)} \quad , \quad E \sim m^{-\varepsilon/(2+\varepsilon)} \tag{2.11}$$

These scaling laws are also applicable for $\varepsilon = 0$, in which case the potential is logarithmic, $V(R) = a \cdot \log R/R_0$.

c) Bottonium [+] etc.

If the linear potential dominates, like in Charmonium, then $\Delta E \sim m^{-1/3}$. Eichten and Gottfried [20] predicted for the Υ system a spacing of $M_{\Upsilon'} - M_{\Upsilon} = 425$ MeV using $M_{\psi'} - M_{J/\psi} = 589$ MeV as input. However, experimentally [6] $M_{\Upsilon'} - M_{\Upsilon} = 556 \pm 3$ MeV which is much closer to $M_{\psi'} - M_{J/\psi}$. Thus the standard Charmonium potential is not the universal potential in QCD. Phenomenologically one is better off with a logarithmic potential [21] because of the constant spacings. However a pure log potential has no justification in QCD. But one can approximate the intermediate $Q\bar{Q}$ potential by a logarithmic one. This has been done by Bhanot and Rudaz [22] with the Ansatz

$$V(R) = \begin{cases} -4/3 \cdot \alpha_s/R & R < R_1 \\ b \cdot \log(R/R_0) \quad \text{for} & R_1 \leq R \leq R_2 \\ a \cdot R & R > R_2 \end{cases} \tag{2.12}$$

and with the requirement of $V(R)$ being continuously differentiable at R_1 and R_2. With a constant α_s for Charmonium and Bottonium, $\alpha_s = 0.31$, and $a = 0.787$ GeV/fm they obtained $M_{\Upsilon'} - M_{\Upsilon} = 560$ MeV. It is amusing to note that this value of a is even in agreement with what one would expect from the old meson spectroscopy.

For a study of very heavy Quarkonia, however, $\alpha_s = \text{const}$ is a bad approximation. One has to take the logarithmic variation of the effective α_s with R

[+] The justification for bottom, i.e. $e_Q = -1/3$, will be given in Chapter 3.

into account, as done by Ono and one of the authors [23]. In this approach the Coulomb potential is modified via Eq. 2.3

$$-\frac{4}{3}\alpha_s(q^2,\lambda^2)\frac{4\pi}{q^2} \quad \xrightarrow{N=3} \quad \simeq -\frac{64\pi^2}{27}\frac{1}{q^2\log(-q^2/\lambda^2)} \tag{2.13}$$

and the Fourier transform becomes [24]

$$V_{AF}(R) = \frac{1}{R}\left\{\frac{-16\pi}{27}\frac{1}{\log(1/R^2\lambda^2 e^{2\gamma})} + \mathcal{O}(\log^{-3})\right\} \tag{2.14}$$

where γ = Euler's constant.

For Charmonium and Bottonium the two potentials give identical predictions. The differences will show up at the next Onium, if its mass is high enough. In Fig. 2.2 the level spacings are shown as functions of the quark mass.

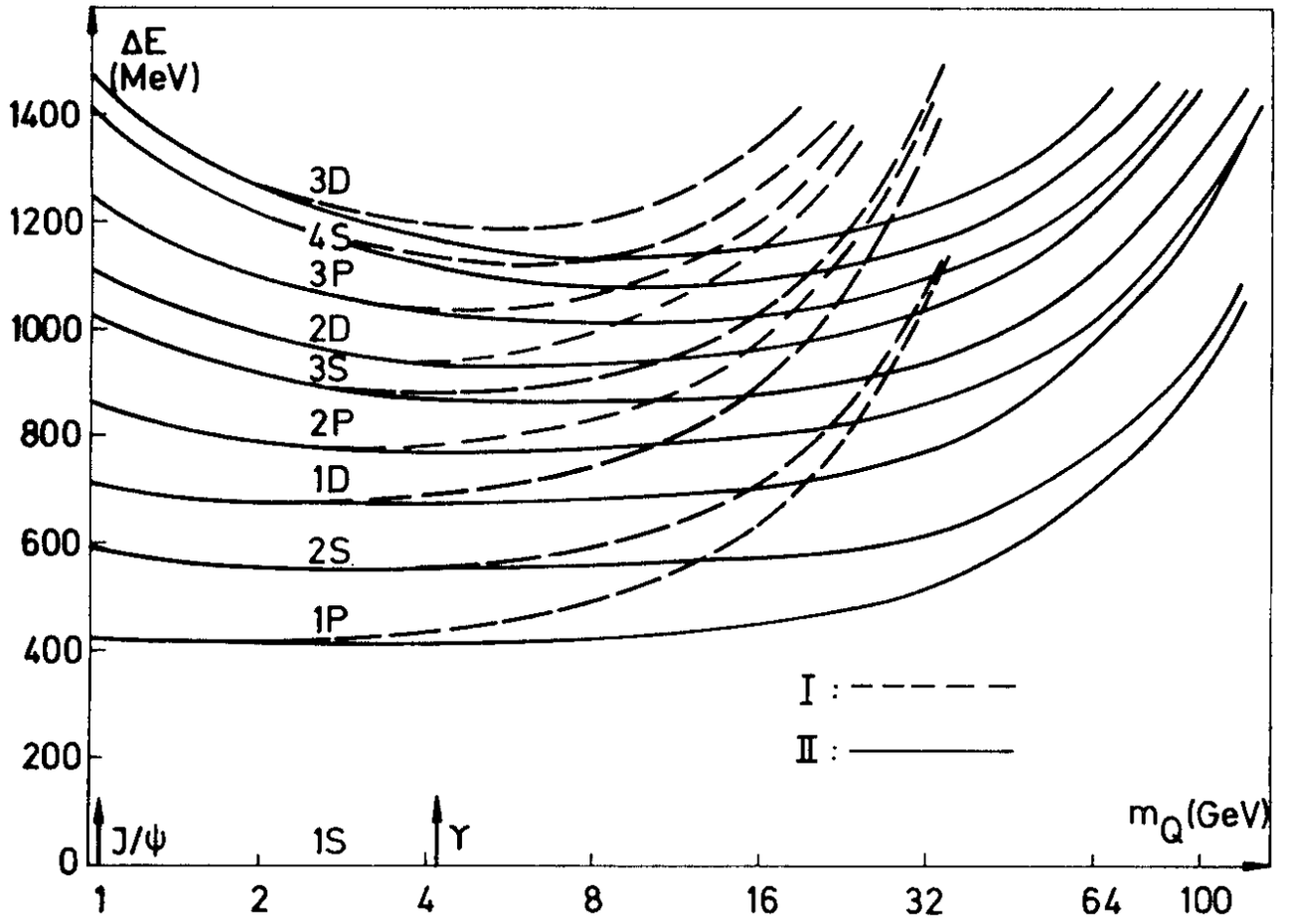

Fig. 2.2. Mass differences to the ground state in model Ref. 23 (full line) and model Ref. 22 (dashed line).

In Fig. 2.3 the reduced leptonic widths are shown. The constancy of $\Gamma_{e\bar{e}}/e_Q^2$

from $\varrho^0(770)$ to $\Upsilon(9.46)$ is a rather interesting fact. But its explanation lies outside the scope of nonrelativistic potential models.

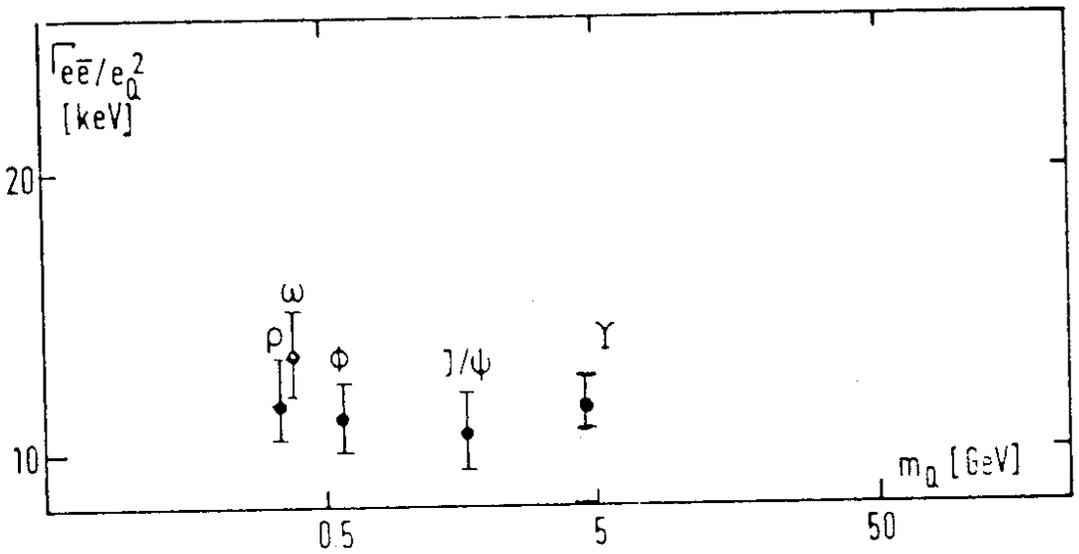

Fig. 2.3. Reduced leptonic decay widths.

Whereas in model I (Ref. 22) $\Gamma_{e\bar{e}}/e_Q^2$ increases for Quarkonia heavier than Υ, Fig. 2.4, so that it will have doubled for $m_{Q\bar{Q}} \simeq 30$ GeV, this increase in model II (Ref. 23) is much slower.

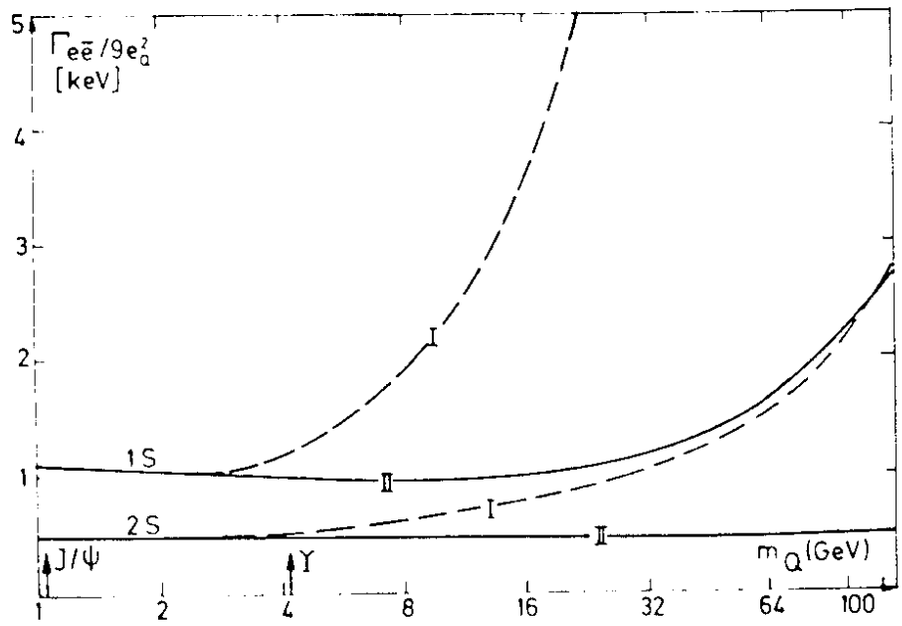

Fig. 2.4. $\Gamma_{e\bar{e}}/9e_Q^2$ as a function of m_Q for model I and II.

The mass of the next quark is an interesting question. In Table 2.1 we give a list of numbers. This list is typical for the speculative character of the predictions.

Threshold in e^+e^- due to the sixth quark:	$M_{threshold} = 21.3$ GeV $M_{n+1} = M_n + 0.7\ n^2$ $M_1 = 0.3$ GeV	H. Lehmann [25]
Bound states of the sixth quark:	$M_{t\bar{t}} = 23.8$ GeV	G.J. Aubrecht II and D.M. Scott [26]
	$M_{Q\bar{Q}} = 28$-29 GeV by the 'factor 3 or π rule': $M_\phi : M_{J/\psi} : M_\Upsilon = 1.02:3.1:9.46$	every third expert [27]
	$M_{Q\bar{Q}} = 40$ GeV	G. Preparata [28]
Current mass of the sixth quark (top quark):	$2m_t = 17.6$, 25.8 GeV	W. Kummer [29]
	$2m_t = 22$, 26, 100 GeV	M.-A. de Crombrugghe [30]
	$2m_t = 27.2$ GeV	H. Georgi and D.V. Nanopoulos [31]
	$2m_t = 28$ GeV	H. Harari, H. Haut and J. Weyers [32]
	$2m_t = 52$ GeV	S. Pakvasa and H. Sugawara [33]
	$2m_t = 54$ GeV	J.D. Bjorken [34]
	$2m_t = 80$ GeV	T.F. Walsh [35]
Current mass of the fourth quark with $e_Q = -1/3$:	$2m_Q = 32 - 40$ GeV	T.F. Walsh [35]

Table 2.1. Predictions for thresholds, bound state masses and current quark masses. We are aware of the fact that we have certainly missed the prediction of one or another of our colleagues.

d) Number of Bound States below Threshold

The higher the mass of the quark the more states are below threshold. Their number can be fairly easy estimated. The condition for lying below threshold is $M_{Q\bar{Q}} < 2M_{Q\bar{q}}$ or with $M_{q_1q_2} = m_{q_1} + m_{q_2} + E_{q_1q_2}$

$$E_{Q\bar{Q}} < 2m_q + 2\,E_{Q\bar{q}} \tag{2.15}$$

The binding of $Q\bar{Q}$ depends on the mass of the heavy quark. The states fall deeper into the potential well with increasing m_Q. For $Q\bar{q}$, on the other hand, the light quark mass (reduced mass) determines the properties of the system. In a very crude first approximation $E_{Q\bar{q}}$ can be taken as a constant and then the threshold is fixed. The number of bound states is obtained semiclassically from the Bohr Sommerfeld quantization condition

$$\int_0^{R_o} dR \sqrt{m_Q\,(E_{thr} - V(R))} = \pi\,(n - 1/4) \tag{2.16}$$

and one finds, since $E_{thr} = V(R_o)$ and R_o become independent of m_Q, [36]

$$n = \frac{1}{4} + \text{const.}\sqrt{m_Q} \tag{2.17}$$

Quigg and Rosner fixed the constant in Charmonium, where n = 2. Fig. 2.6 shows their prediction for heavy quarks. In Bottonium n = 3 is expected and Υ''' should already be a factory for B mesons via $B\bar{B}$ and/or eventually $B\bar{B}^*$, $\bar{B}B^*$. The width of Υ''' may be well below the machine width in e^+e^- annihilation, since the large number of nodes in the radial wave function of Υ''' will suppress its decay into two slowly moving ground state S waves like B or B^*.

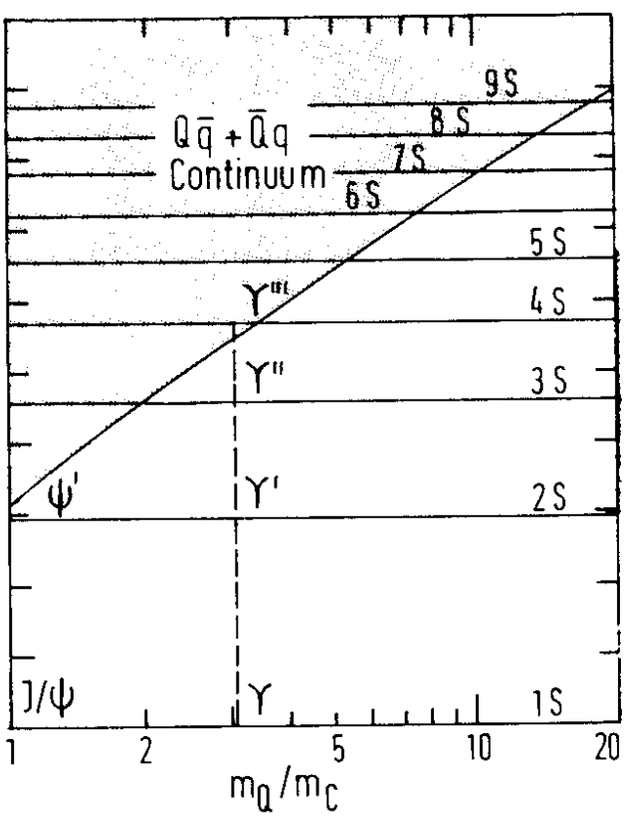

Fig. 2.6. Number of bound states below the strong decay threshold [36].

3. The Charge of the Quarks and Local Duality

The charmed quark and its charge were predicted in 1970. The GIM [3]

mechanism fixes e_c to + 2/3. For the charge of the quark constituing the Υ-system no such strong prediction exists.

Without any theoretical prejudice one would have to wait until one finds the B particles in order to tell the charge. If the combinations with the strange quark $Q\bar{s}$, $\bar{Q}s$ are neutral, $e_Q = -1/3$, if they are charged, $e_Q = 2/3$. In this sense, the discovery of the charged $F^{\pm}(2040)$ meson finally confirmed that $e_c = 2/3$.

From the parton point of view, the charge of the new quark is measured by the step in $R = \sigma_{hadron}/\sigma^{QED}_{\mu\bar{\mu}}$ in e^+e^- annihilation above the new particle threshold: $\Delta R = 1/3$ (4/3) for $e_Q = -1/3$ (2/3). However, we need not go into the continuum, the resonance spikes below threshold already tell us the charges of the quarks. The quantity

$$\frac{1}{\Delta M}\int_{res} dM\, \sigma_M(res \to all) \Big/ \sigma^{QED}_{\mu\bar{\mu}}(q^2=M^2) \equiv \Delta R_{res} \tag{3.1}$$

measures a step ΔR for a given spacing ΔM. With help of the relation

$$\int_{res} dM\, \sigma_M(res \to all) = 6\pi^2\, \Gamma(res \to e^+e^-)/M^2_{res} \tag{3.2}$$

one obtains in the Υ system from [6] $\Gamma(\Upsilon \to e^+e^-) = (1.32 \pm 0.09)\,keV$ and $\Delta M = M_{\Upsilon'} - M_{\Upsilon} = (556 \pm 3)\,MeV$

$$\Delta R_{\Upsilon} = 0.63 \pm 0.04. \tag{3.3}$$

This value of ΔR lies between the values for the two possible charges. If we continue with $\Gamma(\Upsilon' \to e^+e^-) = 0.38^{+}_{-}0.10$ keV and $\Delta M = M_{\Upsilon''}(10.41) - M_{\Upsilon}(10.015) = 0.40$ GeV we obtain

$$\Delta R_{\Upsilon'} = 0.26 \pm 0.07 \tag{3.4}$$

which clearly favours $|e_Q| = 1/3$, i.e. the bottom quark.

Originally specific models predicted specific values for Γ_{ee} [21]. Another way to evaluate the charge of the quark is studying the scaling properties of Γ_{ee} in possible potential models [37]. Also in this approach the decisive evidence for a charge of -1/3 comes from Γ_{ee} of Υ'. A simple continuation of

the observed constancy of $\Gamma_{e\bar{e}}/e_Q^2$ (Fig. 2.3) would give $(e_Q/e_c)^2 = \Gamma_{e\bar{e}}(\mathrm{I})/\Gamma_{e\bar{e}}(\mathrm{J}/\psi)$ and thus $|e_Q| = 1/3$. Potential models predict $\Gamma_{ee}(\Upsilon'') \approx 0.17$ keV. [38]

We shall now demonstrate that a parton type scaling behaviour is a property of a rather general class of potential models. We use Eq. 3.2 and

$$\Gamma(res \rightarrow e^+e^-) = 16\pi\alpha^2 \frac{3e_Q^2}{3} \frac{|\psi_{res}(0)|^2}{M_{res}^2} \tag{3.5}$$

and approximate the mass squared of the n^{th} resonance by

$$M_n^2 \simeq 4m^2 + 4mE_n \tag{3.6}$$

where E_n is the Schrödinger eigenvalue. Semiclassically one can relate the S wave functions at the origin to the spectrum in a rather potential independent way. With

$$\psi_n(\vec{x}) = \frac{1}{\sqrt{4\pi}} \frac{u_n(R)}{R} \quad \text{and} \quad p_n^2 = 2\mu(E_n - V(R)) \tag{3.7}$$

the normalized WKB solution is for finite V(0)

$$u_n(R) = \frac{p_n^{-1/2}(R)}{\left[\int_0^{R_{max}} d\tilde{R}\; p_n^{-1}(\tilde{R})\right]^{1/2}} \cdot \sqrt{2} \cdot \sin\left(\frac{1}{\hbar}\int_0^R d\tilde{R}\, p_n(\tilde{R})\right) \tag{3.8}$$

By differentiating the Bohr-Sommerfeld quantization condition

$$\int_0^{R_{max}} d\tilde{R}\; p_n(\tilde{R}) = \pi\hbar\,(n + const.) \tag{3.9}$$

with respect to n, one obtains the relation [39]

$$4\pi^2 |\psi_n(0)|^2 = \sqrt{2\mu E_n/\hbar^2} \cdot \frac{d(2\mu E_n/\hbar^2)}{dn} \tag{3.10}$$

Insertion of this relation into Eq.s 3.5 and 3.2 leads to [40]

$$\frac{1}{\Delta M}\int_{res} dM\, \sigma_M(res \rightarrow all) = \frac{4\pi\alpha^2}{3M^2} 3e_Q^2 \cdot \frac{3}{2}\sqrt{1 - 4m^2/M^2}\,. \tag{3.11}$$

For comparison the parton model cross section reads

$$\sigma_{parton}(q^2) = \frac{4\pi\alpha^2}{3q^2} 3e_Q^2 \left(1 + \frac{2m^2}{q^2}\right)\sqrt{1 - 4m^2/q^2}\,. \tag{3.12}$$

Thus even with the nearly correct threshold factors ($3/2 \simeq 1 + 2m^2/q^2$) the resonances reproduce in an approximate way the parton behaviour: this is called local q^2 duality. For Charmonium Fig. 3.1 shows the smoothened resonances for four different potential models [41] and the curve corresponds to Eq. 3.11 with the current quark mass $m_c = 1.25$ GeV.

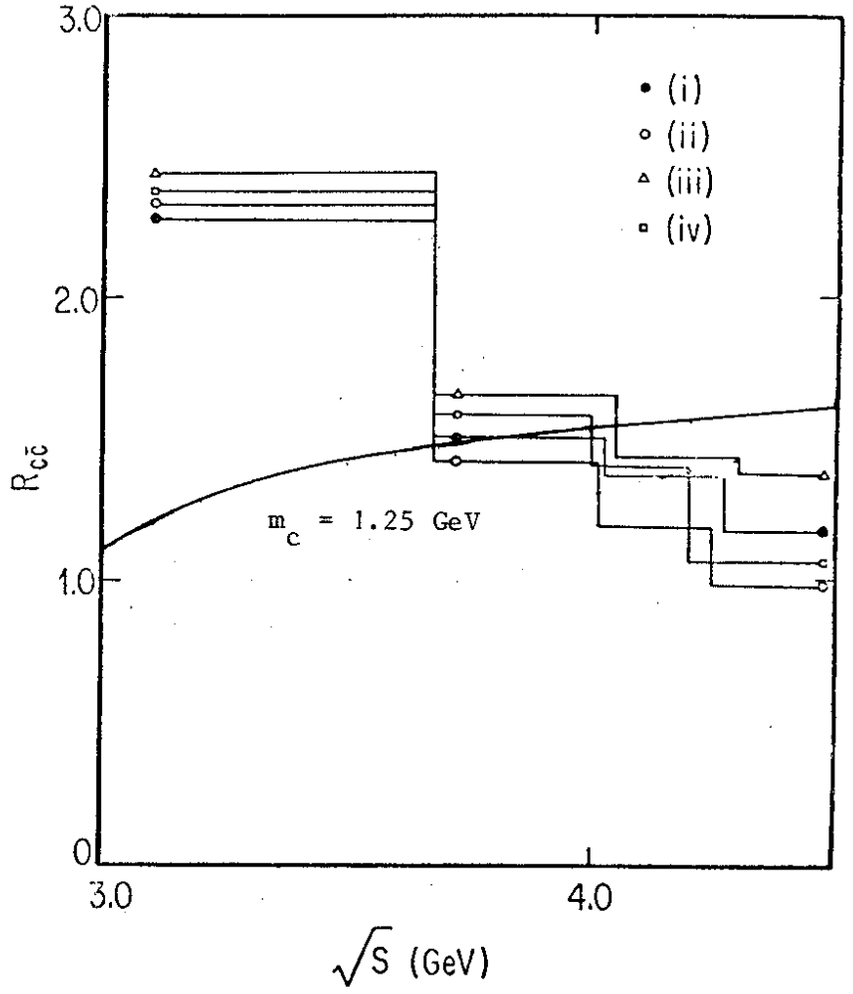

Fig. 3.1. From Ref. 40. (i) - (iv) denote the four potential models of Ref. 41.

4. Level Splittings (Fine and Hyperfine Structure)

In the physical spectrum the Schrödinger states are split up due to spin interactions. In this Chapter we want to compare the magnitude of these splittings with the simplest Ansatz we can imagine, the Fermi Breit Hamiltonian [42]. These higher order corrections are relativistic kinematic corrections and spin corrections:

$$H = H^o + H^{rel} + H^{spin} \tag{4.1}$$

The spin corrections have three contributions:

$$\text{spin-orbit:} \quad H^{LS} = \frac{2}{m_Q^2} \vec{L}\cdot\vec{S} \left[\frac{1}{R}\frac{d}{dR}\right]\left(V_{AF}(R) - \frac{1}{4}V(R)\right)$$

$$\text{tensor:} \quad H^{T} = \frac{-1}{12 m_Q^2}\left(3\vec{\sigma}_1\cdot\hat{R}\vec{\sigma}_2\cdot\hat{R} - \vec{\sigma}_1\cdot\vec{\sigma}_2\right)\left[\frac{d^2}{dR^2} - \frac{1}{R}\frac{d}{dR}\right]V_{AF}(R) \qquad (4.2)$$

$$\text{spin-spin:} \quad H^{SS} = \frac{1}{6 m_Q^2}\,\vec{\sigma}_1\cdot\vec{\sigma}_2\;\Delta V_{AF}(R)$$

Here $\vec{\sigma}_i/2$ is the quark spin, $S = 1/2(\vec{\sigma}_1+\vec{\sigma}_2)$ the meson spin, $\vec{L}$ its angular momentum, R the interquark distance. For the potential V(R) we take the simplest ansatz $V = V_{AF} + V_C$ with only $V_{AF}(R)$ being spin-dependent. Nevertheless, the spin-independent V_C contributes to the spin orbit interaction due to the relativistic kinematic effect of the Thomas precession [43], represented by the tem $-1/4\ V(R)$ in H^{LS}(4.2). In Quarkonium this additional Thomas precession decreases the spin orbit splittings and it decreases $R_P = \Delta M(^3P_2 - {}^3P_1)/\Delta M(^3P_1 - {}^3P_0)$. While in Positronium, where $V(R)\sim -1/R \sim V_{AF}(R)$, $R_P = 0.8$, the experimental value in Charmonium is $R_P = 0.5$. [1]

We are confident that the Fermi-Breit Hamiltonian (4.2) is not a too bad approximation. As an example let us consider the part of the relativistic corrections due to the kinetic energy of the quarks. This correction is $\langle(\vec{p}^2)^2/4m_Q^3\rangle \approx E_{kin}\langle\beta^2/4\rangle$. Up to β^2 of 0.4 the relativistic kinetic energy correction is less than 10 %. The β^2 one obtains in Charmonium calculations is 0.2 to 0.3 for J/ψ and 0.27 to 0.4 for ψ' varying m_c from 1.6 to 1.16 GeV.

Let us now compare experiment with the predictions from (4.2). The three P waves of Charmonium are quite well established, as shown in Table 4.1:

Table 4.1:

State	$^3P_2(2^{++})$	$^3P_1(1^{++})$	$^3P_0(0^{++})$	center of gravity
mass [GeV]	3.552	3.508	3.415	3.522

The P wave splittings can be parametrized as

$$\langle H^{LS}\rangle = A\langle\vec{L}\cdot\vec{S}\rangle \quad , \quad \langle H^{T}\rangle = B\langle T\rangle \qquad (4.3)$$

where the tensor operator $T \equiv 3\vec{\sigma}_1\cdot\hat{R}\vec{\sigma}_2\cdot\hat{R} - \vec{\sigma}_1\cdot\vec{\sigma}_2$. The expectation values of $\vec{L}\cdot\vec{S}$ and T can be found in textbooks on Quantum Mechanics [44]. They are displayed

in Table 4.2. A Charmonium analysis with the experimental masses of Table 4.1

j	$\langle \vec{L}\cdot\vec{S}\rangle$	$\langle T\rangle$
$\ell+1$	ℓ	$-2\ell/(2\ell+3)$
ℓ	-1	2
$\ell-1$	$-(\ell+1)$	$-2(\ell+1)/(2\ell-1)$

Table 4.2.

yields for A and B

$$A \simeq 34 \text{ MeV}, \qquad B \simeq 10 \text{ MeV} \tag{4.4}$$

We obtain from (4.2) for the standard Charmonium potential

$$A = \frac{2}{m_Q^2}\langle \alpha_s R^{-3} - \frac{1}{4} a R^{-1}\rangle \ ,$$
$$B = \frac{1}{3m_Q^2}\langle \alpha_s R^{-3}\rangle \ . \tag{4.5}$$

We see that the spin dependence from the one gluon exchange (V_{AF}) is governed by $\langle R^{-3}\rangle$ while the Thomas precession is governed by $\langle R^{-1}\rangle$. Taking our $\alpha_s = 0.4$, $m_c^{-1}\langle R^{-3}\rangle \simeq 0.07$ GeV^2 and $\langle R^{-1}\rangle \simeq 0.4$ GeV from numerical fits we obtain the values of A and B given in Table 4.3 for two different values of m_c. By

m_c [GeV]	1.6	1.1
A [MeV]	35-12=23	56-32=24
B [MeV]	6	9

Table 4.3: A and B from numerical fits. In row A the contribution from the Thomas precession is 12 and 32 MeV respectively.

comparison of Table 4.3 with Eq. (4.4) we see that we are in the right ball park. We could not have expected a better agreement from our crude approximation!

Let us now try the spin-spin interaction which arises from the short

range one gluon exchange V_{AF} alone. The relevant term in the Fermi-Breit Hamiltonian (4.2) was

$$H^{SS} = \frac{1}{6m_Q^2}\,\vec{\sigma}_1\cdot\vec{\sigma}_2\,\Delta V_{AF}(R) \tag{4.6}$$

Because $\Delta V_{AF}(R) \sim \Delta\left(\frac{-1}{R}\right) = 4\pi\delta(R)$ the integral over the wave functions becomes trivial and with $\vec{\sigma}_1\cdot\vec{\sigma}_2 = 2\vec{S}^2 - 3$ we have

$$\langle H^{SS}\rangle = \frac{4}{3}\alpha_S\,4\pi\,\frac{1}{6m_Q^2}\,(2\vec{S}^2-3)\,|\psi(0)|^2 \tag{4.7}$$

It is clear that (4.7) is an overestimate because the one gluon exchange potential has a weaker singularity at the origin than the $-1/R$ potential.

Taking $|\psi(0)|^2$ from Γ_{ee} via Eq. (2.5) and α_S from Eq. (2.4) gives us for the splittings

$$\begin{aligned} M(1^3S_1) - M(1^1S_0) &\simeq 70\ \text{MeV}\ (M_{J/\psi}/2m_c)^2 \\ M(2^3S_1) - M(2^1S_0) &\simeq 35\ \text{MeV}\ (M_{\psi'}/2m_c)^2 \end{aligned} \tag{4.8}$$

Trying to identify $\eta_c(1^1S_0) \equiv X(2.83)$ means ≈ 70 MeV $\equiv$ 250 MeV, $\eta_c'(2^1S_0) \equiv \chi(3.45)$ means ≈ 35 MeV $\equiv$ 230 MeV, or $\eta_c'(2^1S_0) \equiv \chi(3.59)$ means ≈ 35 MeV $\equiv$ 80 MeV. Many solutions have been proposed to solve this puzzle, among these are instanton effects [45] and an anomalous colour magnetic moment of the c-quark [46]. The simplest solution might be that the $|\psi(0)|^2$ in Eq. (2.5) and in (4.7) are different objects. The next order correction to $|\psi(0)|^2$ in (2.5) comes in through a transverse gluon exchange between the two quark lines before annihilation. It yields a factor [18]

$$\left(1 - \frac{16\alpha_S}{3\pi}\right) \tag{4.9}$$

which in no case is small. But before continuing this discussion let us wait for estimates of some decay rates involving the pseudoscalars. Then we will find that we have much more severe problems which question the identifications above.

Let us now discuss the P and D wave splittings for heavier Quarkonia in models I (Ref. 22) and II (Ref. 23). Fig. 4.1 shows the mass difference

$\Delta M(^3P_2 - {}^3P_0)$ and the ratio $R_P = \Delta M(^3P_2 - {}^3P_1)/\Delta M(^3P_1 - {}^3P_0)$ as a function of the quark mass. The decrease of the overall splittings can be estimated

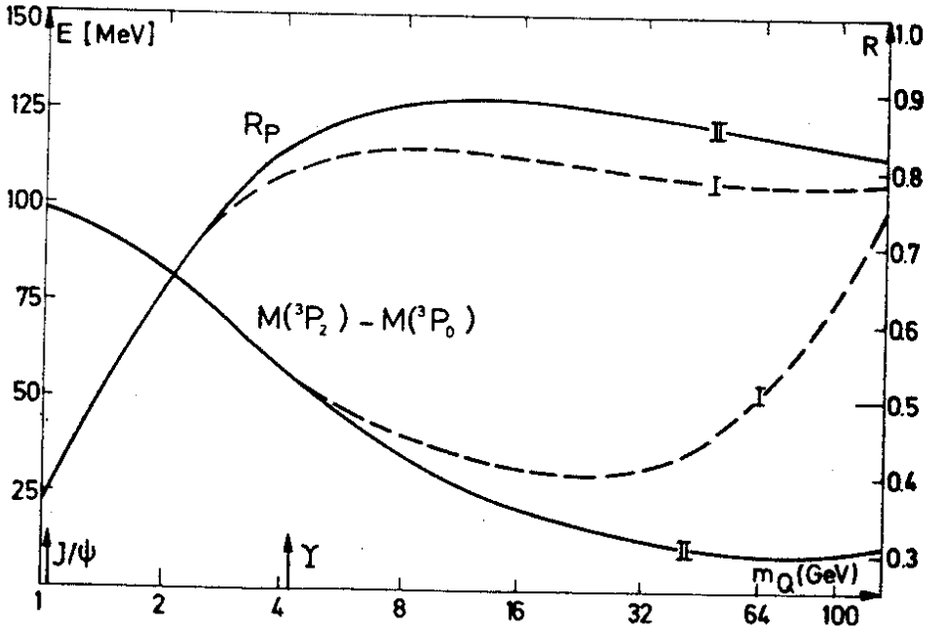

Fig. 4.1. The mass difference $\Delta M(^3P_2 - {}^3P_0)$ and the ratio R_P as a function of m_Q in model I and II.

from the scaling behaviour of the radius R (2.11) in intermediate potential regimes, where the potential is logarithmic, $R^{-3} m_Q^{-2} \sim m_Q^{-1/2}$, compare Eq.s (4.5). The Thomas precession contribution from confinement, however, decreases much faster like $R^{-1} m_Q^{-2} \sim m_Q^{-3/2}$. The sharp rise of R_P between 1 and 8 GeV quark mass is due to this difference in the scaling behaviour. The increase of the splittings above $M(Q\bar{Q}) \simeq 200$ GeV (model II) is due to the Coulomb like potential at short distances for which all mass differences have to scale like m_Q, the better the smaller Λ/m_Q is. If QCD were not asymptotic free but pure Coulombic at short distances, the increase would show up much earlier, namely above $M(Q\bar{Q}) \simeq 30$ GeV (model I). With asymptotic freedom the ratio R_P approaches the asymptotic Coulomb value of 0.8 from above, because the spin dependent potential is weaker than Coulomb.

For the D wave masses we also parametrize like in Eq. (4.3) with $\langle \vec{L}\vec{S} \rangle$ and $\langle T \rangle$ again given in Table 4.2. The coefficients A, B and $R_D = \Delta M(^3D_3 - {}^3D_2)/\Delta M(^3D_2 - {}^3D_1)$ are shown in Fig. 4.2 as functions of the quark mass. The interesting thing is the change of sign of A for $m_Q \simeq 1.4$ GeV which in case of small m_c leads to an inversion of the D wave multiplet in Charmonium. A similar inversion of the P wave multiplet of the charmed mesons, D_P^*, F_P^*, has been predicted by Schnitzer [47].

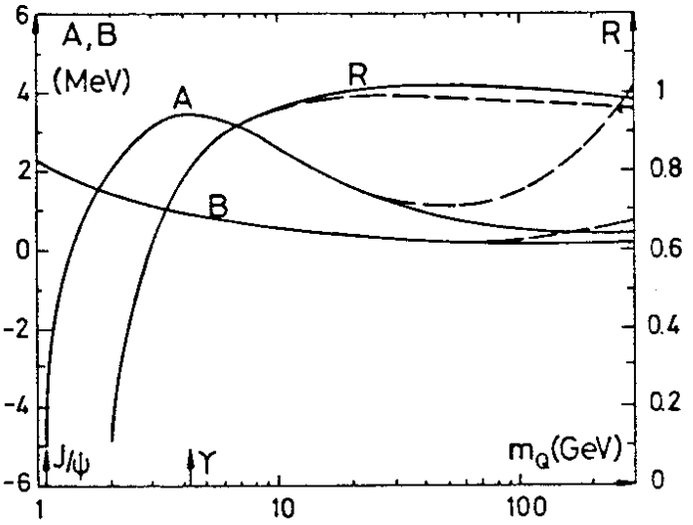

Effects of this Thomas precession also seem to show up in the baryon spectrum, where a phenomenological description of the splittings indicates that the net spin orbit splittings are small. In a potential model the $\vec{L}\cdot\vec{S}$ term and the Thomas precession have to cancel [48].

Fig. 4.2. The parameters A,B,C and the ratio R_D for Quarkonium D waves as functions of m_Q in model I (- - -) and I (———).

5. How to Find the Levels

The best place to study the levels of Quarkonia is in e^+e^- annihilation. There the vector states are produced via one-photon annihilation. The cross section is given by

$$\sigma(e^+e^- \longrightarrow V \longrightarrow f) = \frac{12\pi\,\Gamma_{V\to e^+e^-}\cdot\Gamma_{V\to f}}{(q^2-M_V^2)^2+M_V^2\,\Gamma_{tot}^2} \tag{5.1}$$

which yields for a narrow resonance

$$\int_{res} dM\ \sigma(e^+e^- \longrightarrow V \longrightarrow f) = 6\pi^2\,\frac{\Gamma_{V\to e^+e^-}}{M_V^2}\,\mathcal{B}_{V\to f} \tag{5.2}$$

From the 1^{--} $Q\bar{Q}$ states one can reach the lower levels by photonic and/or hadronic transitions.

The C = + levels can be reached by one photon transitions. In the next Chapter we shall discuss the electric and magnetic dipole transitions. The C = - states can be reached from the vector mesons via two photon emission, preferentially via a C = + state.

In Fig. 5.1 the hadronic transitions via $\pi\pi$, η, 3π are shown for Bottonium.

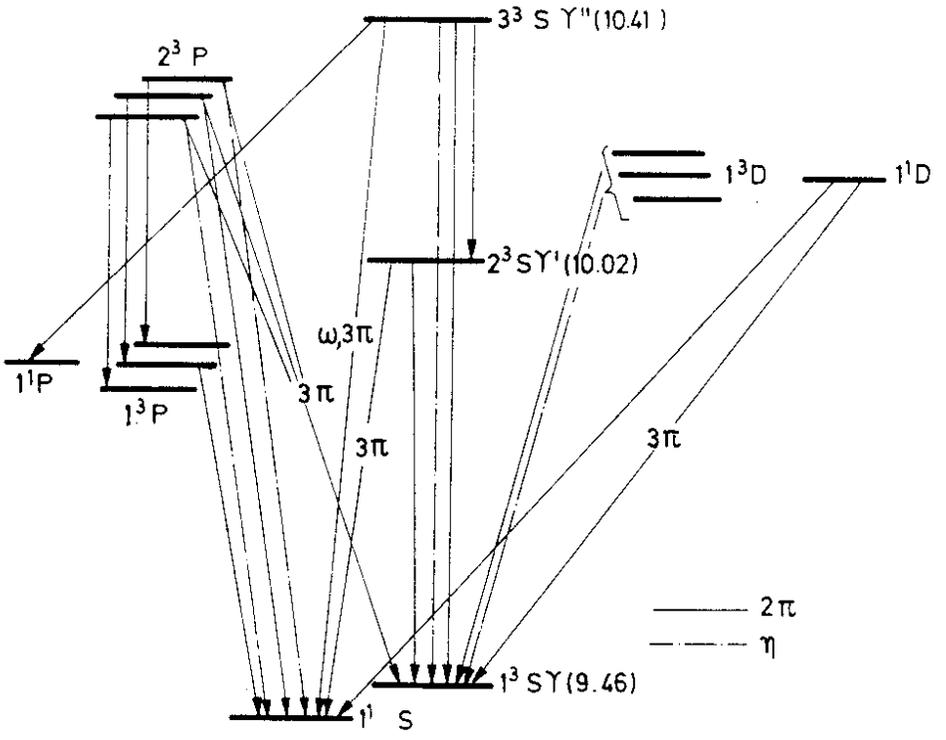

Fig. 5.1. Hadronic transitions in Bottonium. The Figure is an updated version of that of Ref. 20.

A rather important transition to be looked for is the decay $3^3S_1(\Upsilon'') \to 1^1P_1(1^{+-}) + \varepsilon(\pi\pi)$. It would reveal the $^1P_1$ state, whose existence is difficult to prove in Charmonium, where one had to look for $\Psi'(3.7) \to 1^{+-} + \gamma\gamma$. Finding of the 1^1P_1 state is important because its mass allows to determine, whether there are long range spin-spin correlations or not. In our Ansatz for the Hamiltonian we only had short range spin-spin forces. They do not act on P waves and therefore the 1^1P_1 state is degenerate with the c.o.g. of the 1^3P_j states. A long range spin-spin force [49], however, would act on the P waves and would lift this degeneracy.

According to Gottfried [50] the hadronic cascade decays can be understood as radiative gluon transitions which can be subject to a multipole expansion similar to electromagnetic radiation. While the expansion in $(kR/2)^2$ might converge, the expansion in α_s/π needs not. The distances involved in the process are of the order of the wave function radius and α_s will be large. This is the essential reason why we do not expect to be able to calculate absolute rates for gluon radiation. But we might be able to derive selection rules

and the scaling behaviour. The typical example is [51]

$$\Gamma(Q\bar{Q}_2 \longrightarrow Q\bar{Q}_1 + \lambda) \sim m_Q^{-2} \tag{5.3}$$

for any two $Q\bar{Q}$ states of the same flavour Q and λ any state of light quarks, provided $Q\bar{Q}_1$ and $Q\bar{Q}_2$ have the same parity, $\Delta L = 0$ or 2 and $\Delta S = 0$. If this scaling law is already valid in Charmonium, then $\Gamma(\psi' \to J/\psi\,\pi\pi) \simeq 100$ keV implies $\Gamma(\Upsilon' \longrightarrow \Upsilon\,\pi\pi) \simeq 10$ keV.

In a recent paper, Billoire, Lacaze, Morel and Navelet [52] have investigated the cascade $2^3S_1(Q\bar{Q}) \to 1^3S_1(Q\bar{Q})$ + hadrons. They constrain themselves to the lowest order in α_s and kR ("two gluon colour electric dipole emission") and project out the final spin states. They are able to roughly reproduce the experimentally observed $\pi\pi$ spectrum in $\psi' \to J/\psi\,\pi\pi$, see Fig. 5.2. However, in this approximation the transition $2^3S_1(Q\bar{Q}) \to 1^3S_1(Q\bar{Q}) + \eta$ is zero because the gluon momenta are neglected. (η is emitted with $\ell = 1$, but zero momentum gluons cannot carry angular momentum).

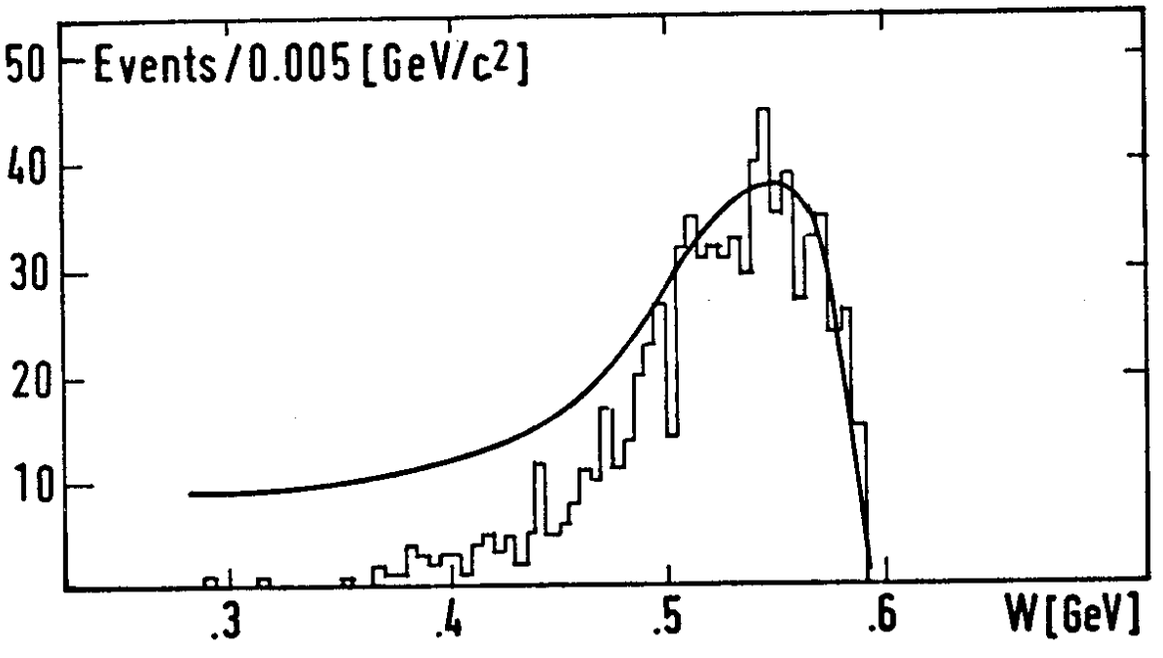

Fig. 5.2. Comparison of the 0^+ spectrum for $\psi' \to J/\psi + 2q$ to the experimental data for $\psi' \to J/\psi\,\pi\pi$. The spectrum corrected for acceptance is normalized to the observed events in the peak region. The disagreement on the low mass side is due to phase space and the absence of an Adler zero in the matrix element of Ref. 52. [53]

6. Photon Transitions and Sum Rules

For photon wave lengths long against the bound state size one can do a multipole expansion. The widths are [54]

$$\Gamma \sim \alpha e_Q^2 \begin{Bmatrix} k^3 R^2 \\ k^3 m_Q^{-2} \end{Bmatrix} \left(\frac{kR}{2}\right)^{2(n-1)} \quad \text{for} \begin{Bmatrix} E_n \\ M_n \end{Bmatrix} \text{transitions.} \tag{6.1}$$

Here k is the photon wave number, R the bound state radius in the reduced system. The expansion parameter is $(kR/2)^2$ and is roughly 1/4 to 3/100 in Charmonium, thus justifying the multipole expansion.

a) Electric Dipole Transitions and E1 Sum Rules

In Quarkonium the formula for an electric dipole transition (E1) is [54]

$$\Gamma^{E1}(Q\bar{Q} \rightarrow \gamma \cdot Q\bar{Q}) = \frac{4}{3} \alpha e_Q^2 k^3 |\vec{x}_{fi}|^2 \tag{6.2}$$

where $\vec{x}_{fi}$ is the matrix element of the dipole operator.

There are many corrections to the naive formula:

i) higher multipoles which are at most 5 % in ψ' decays;

ii) interference of the finite wave length of the photon field e^{ikR} with the bound state wave function. Okun and Voloshin [55] have shown that these corrections amount to at most 5 % in Charmonium;

iii) relativistic corrections, consisting of a) relativistic corrections to the wave functions, b) the interaction of the quark magnetic moment with the electric vector of the photon field, the last correction gives factors 1.0 to 0.6 [55]; c) the recoil corrections have been found to be + 20 % in a relativistic model [56].

The radiative E1 widths of the standard Charmonium model are shown in Fig. 6.1. The numbers in brackets are the model widths with corrections of type iii b). All this indicates that the model numbers are only correct up to a factor two.

There are two kinds of electric dipole sum rules, the so called Thomas - Reiche - Kuhn (TRK) sum rule (SR) and the Wigner SR [57]. They were rediscovered for Charmonium by Jackson [58]. Both SR's apply to the dipole matrix element (6.2) without corrections. The SR's are derived from Heisenberg's uncertainty relation

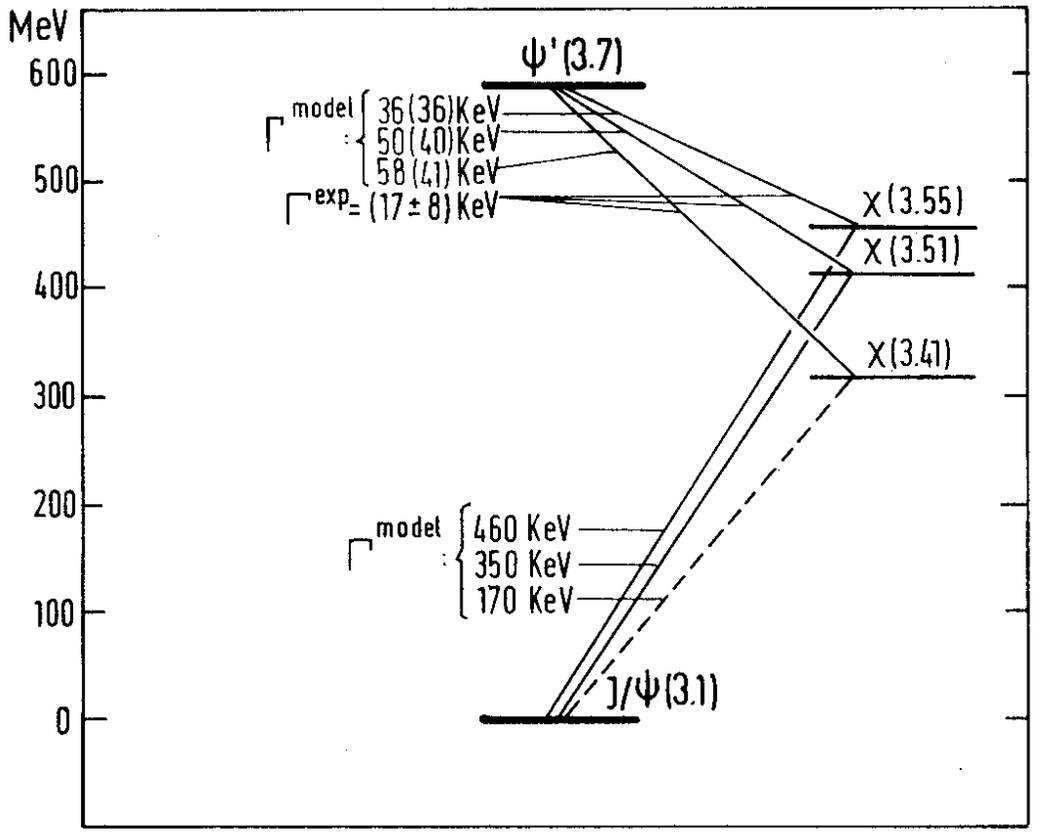

Fig. 6.1. E1 transitions in Charmonium. Model widths are calculated via Eq.s (6.11,12). The numbers in brackets are the corrections of type iii,b).

$$\left[\vec{x}, \vec{p}\right] = 3i \qquad (\hbar = c = 1) \tag{6.3}$$

In a static $Q\bar{Q}$ potential without velocity dependent terms, we can replace $\vec{p}$ via the equation of motion

$$\vec{p} = i \frac{m_Q}{2} \left[H^0, \vec{x}\right] \tag{6.4}$$

After taking the expectation value in a state $|i\rangle$ and inserting a complete set of states $|f\rangle$ the replacement of $\vec{p}$ leads to

$$\sum_f (E_f^0 - E_i^0) |\vec{x}_{fi}|^2 = \frac{3}{m_Q} \tag{6.5}$$

The number of final states is restricted by selection rules. In an arbitrary static potential $\Delta\ell = \pm 1$ for dipole transitions. In a harmonic oscillator

potential, however, the number of final states is further restricted by the oscillator selection rule: The change of the number of radial nodes Δr is either 0 or $-\Delta\ell$. This fact is called saturation of the SR by the harmonic oscillator.

To derive the Wigner SR we recall Eq. (6.3) which can be written as

$$\sum_f \langle i|\vec{x}|f\rangle\langle f|\vec{p}|i\rangle - \langle i|\vec{p}|f\rangle\langle f|\vec{x}|i\rangle = 3i \tag{6.6}$$

The angular selection rule now enables us to project out the final states with $\Delta\ell = +1$ and those with $\Delta\ell = -1$. After some elaborate algebra one arrives at two SR's [57]:

$$\sum_{f,\ell-1} (E_f^\circ - E_i^\circ)\,|\vec{x}_{fi}|^2 = \frac{-\ell(2\ell-1)}{2\ell+1}\cdot\frac{1}{m_Q} \tag{6.7a}$$

$$\sum_{f,\ell+1} (E_f^\circ - E_i^\circ)\,|\vec{x}_{fi}|^2 = \frac{(\ell+1)(2\ell+3)}{2\ell+1}\cdot\frac{1}{m_Q} \tag{6.7b}$$

which of course add up to Eq. (6.5). We have gained two things: first the number of final states on the l.h.s. of (6.7) is smaller than in the TRK SR, and second, (6.7a) has a negative sign which will be very helpful.

b) Explicit Transition Rates and Bounds

To write down the rates it is convenient to express the dipole operator of Eq. (6.2) through the radial operator $R_{f,i}$ [59]

$$\Gamma(\tau,\ell,s,j \longrightarrow \tau',\ell',s,j') = \frac{4\alpha e_Q^2}{3} k^3 (2j'+1) \begin{Bmatrix} \ell' j' s \\ j \ell 1 \end{Bmatrix}^2 |\langle\tau',\ell'\|\times\|\tau,\ell\rangle|^2 \tag{6.8}$$

with

$$\begin{aligned} \langle\tau',\ell-1\|\times\|\tau,\ell\rangle &= i\sqrt{\ell}\int_0^\infty R^2 dR\; R_{\tau',\ell-1}(R)\cdot R\cdot R_{\tau,\ell}(R) \equiv i\sqrt{\ell}\,R_{f,i} \\ \langle\tau',\ell+1\|\times\|\tau,\ell\rangle &= -i\sqrt{\ell+1}\int_0^\infty R^2 dR\; R_{\tau',\ell+1}(R)\cdot R\cdot R_{\tau,\ell}(R) \equiv -i\sqrt{\ell+1}\,R_{f,i} \end{aligned} \tag{6.9}$$

The matrix element $|\vec{x}_{fi}|$ of the sum rules Eq.s (6.5,7) does not involve quark

spin. It is related to $\langle r', \ell' \| x \| r, \ell \rangle$ by

$$\sum_{m'} |\langle r', \ell', m' | \vec{x} | r, \ell, m \rangle|^2 = \frac{1}{2\ell+1} |\langle r', \ell' \| x \| r, \ell \rangle|^2 \tag{6.10}$$

We can now write down rates and bounds. In Fig. 6.2 we show the quark spin triplet E1 transitions for Bottonium. Transitions for which there is an upper and/or lower bound are labelled by the formula numbers.

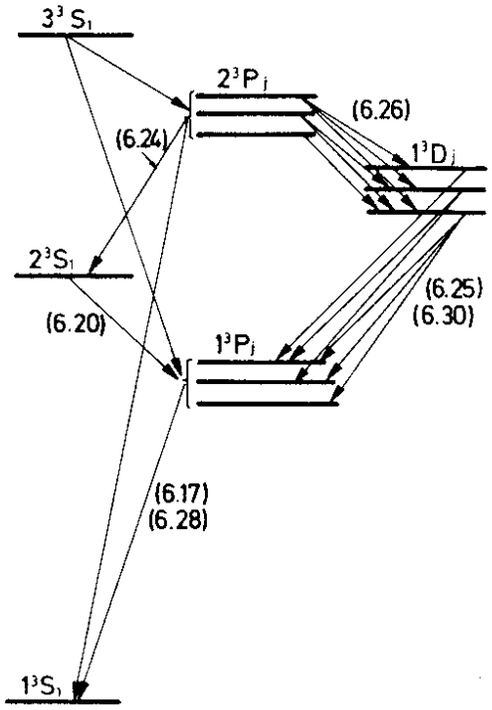

Fig. 6.2. E1 transitions in Bottonium. The numbers in brackets indicate formulae for upper and lower bounds.

The transition rates are:

$$\Gamma(^3P_j \longrightarrow \gamma\, ^3S_1) = \frac{4}{9} \alpha e_Q^2 k^3 |R_{S,P}|^2 \tag{6.11}$$

$$\Gamma(^3S_1 \longrightarrow \gamma\, ^3P_j) = \frac{4}{3} \frac{2j+1}{9} \alpha e_Q^2 k^3 |R_{P,S}|^2 \tag{6.12}$$

$$\Gamma(^3P_j \longrightarrow \gamma\, ^3D_{j'}) = \frac{8}{3} (2j'+1) \alpha e_Q^2 k^3 \begin{Bmatrix} 2 & j' & 1 \\ j & 1 & 1 \end{Bmatrix}^2 |R_{D,P}|^2 \tag{6.13}$$

$$\Gamma(^3D_j \longrightarrow \gamma\, ^3P_{j'}) = \frac{8}{3} (2j'+1) \alpha e_Q^2 k^3 \begin{Bmatrix} 1 & j' & 1 \\ j & 2 & 1 \end{Bmatrix}^2 |R_{P,D}|^2 \tag{6.14}$$

$$\left\{ \begin{matrix} 2 & j' & 1 \\ j & 1 & 1 \end{matrix} \right\}^2 = \left\{ \begin{matrix} 1 & j & 1 \\ j' & 2 & 1 \end{matrix} \right\}^2 = \frac{1}{900} \times$$

j \ j'	1	2	3
0	100	0	0
1	25	45	0
2	1	9	36

(6.15)

The TRK SR (6.5) gives us as a bound

$$(E^0_{1P} - E^0_{1S}) |R_{1P,1S}|^2 \leq \frac{3}{m_Q} \tag{6.16}$$

which implies an upper bound on 1P → 1S

$$\Gamma(1^3P_j \longrightarrow \gamma 1^3S_1) \leq \frac{4}{9} \alpha e_Q^2 \cdot \frac{k^3}{k^{(0)}} \cdot \frac{3}{m_Q} \tag{6.17}$$

For $\ell = 1$ in the initial state the first two terms of (6.7a) give

$$(E^0_{2S} - E^0_{1P}) |R_{2S,1P}|^2 + (E^0_{1S} - E^0_{1P}) |R_{1S,1P}|^2 \leq \frac{-1}{m_Q} \tag{6.18}$$

With (6.16) this results in

$$(E^0_{2S} - E^0_{1P}) |R_{2S,1P}|^2 \leq \frac{2}{m_Q} \tag{6.19}$$

and leads to the upper bound

$$\Gamma(2^3S_1 \longrightarrow \gamma 1^3P_j) \leq \frac{4}{3} \frac{2j+1}{9} \alpha e_Q^2 \frac{k^3}{k^{(0)}} \frac{2}{m_Q} . \tag{6.20}$$

In a similar way we obtain

$$(E^0_{2P} - E^0_{2S}) |R_{2P,2S}|^2 \leq \frac{3}{m_Q} + (E^0_{2S} - E^0_{1P}) |R_{2S,1P}|^2 \leq \frac{5}{m_Q} \tag{6.21}$$

$$(E^0_{1D} - E^0_{1P}) |R_{1D,1P}|^2 \leq \frac{5}{m_Q} \tag{6.22}$$

$$(E^0_{2P} - E^0_{1D}) |R_{2P,1D}|^2 \leq \frac{-3}{m_Q} + (E^0_{1D} - E^0_{1P}) |R_{1P,1D}|^2 \leq \frac{2}{m_Q} \tag{6.23}$$

and thus upper bounds on the widths:

$$\Gamma(2^3P_j \to \gamma 2^3S_1) \leq \frac{4}{9}\alpha e_Q^2 \frac{k^3}{k^{(0)}} \frac{5}{m_Q} , \tag{6.24}$$

$$\Gamma(1^3D_j \to \gamma 1^3P_{j'}) \leq \frac{8}{3}(2j'+1)\alpha e_Q^2 \begin{Bmatrix} 1 & j' & 1 \\ j & 2 & 1 \end{Bmatrix}^2 \frac{k^3}{k^{(0)}} \frac{5}{m_Q} , \tag{6.25}$$

$$\Gamma(2^3P_j \to \gamma 1^3D_{j'}) \leq \frac{8}{3}(2j'+1)\alpha e_Q^2 \begin{Bmatrix} 2 & j' & 1 \\ j & 1 & 1 \end{Bmatrix}^2 \frac{k^3}{k^{(0)}} \frac{2}{m_Q} . \tag{6.26}$$

Next, we write (6.18) as

$$(E^0_{1P} - E^0_{1S})|R_{1S,1P}|^2 \geq \frac{1}{m_Q} + (E^0_{2S} - E^0_{1P})|R_{2S,1P}|^2 \tag{6.27}$$

and obtain by 'inverting' (6.20) the lower bound

$$\Gamma(1^3P_j \to \gamma 1^3S_1) \geq \frac{4}{9}\alpha e_Q^2 \frac{k^3}{k^{(0)}} \frac{1}{m_Q} + \frac{3}{2j+1} \frac{k^3_{1P,1S}\, k^{(0)}_{2S,1P}}{k^3_{2S,1P}\, k^{(0)}_{1P,1S}} \Gamma^{exp}(2^3S_1 \to \gamma 1^3P_j) \tag{6.28}$$

Similarly we obtain from (6.23)

$$(E^0_{1D} - E^0_{1P})|R_{1P,1D}|^2 \geq \frac{3}{m_Q} + (E^0_{2P} - E^0_{1D})|R_{2P,1D}|^2 \tag{6.29}$$

and thus the lower bound on the width

$$\Gamma(1^3D_j \to \gamma 1^3P_{j'}) \geq \frac{8}{3}(2j'+1)\alpha e_Q^2 \begin{Bmatrix} 1 & j' & 1 \\ j & 2 & 1 \end{Bmatrix}^2 \frac{k^3}{k^{(0)}} \frac{3}{m_Q} + \tag{6.30}$$

$$+ \frac{(2j'+1)\begin{Bmatrix} 1 & j' & 1 \\ j & 2 & 1 \end{Bmatrix}^2}{(2j''+1)\begin{Bmatrix} 2 & j'' & 1 \\ j'' & 1 & 1 \end{Bmatrix}^2} \frac{k^3_{1D,1P}\, k^{(0)}_{2P,1D}}{k^3_{2P,1D}\, k^{(0)}_{1D,1P}} \cdot \Gamma^{exp}(2^3P_{j''} \to \gamma 1^3D_{j''}) .$$

In Fig. 6.3 we give the upper bounds for Bottonium using $m_b = 4.6$ GeV. We neglect the splittings and restrict ourselves to states with $j = 1$.

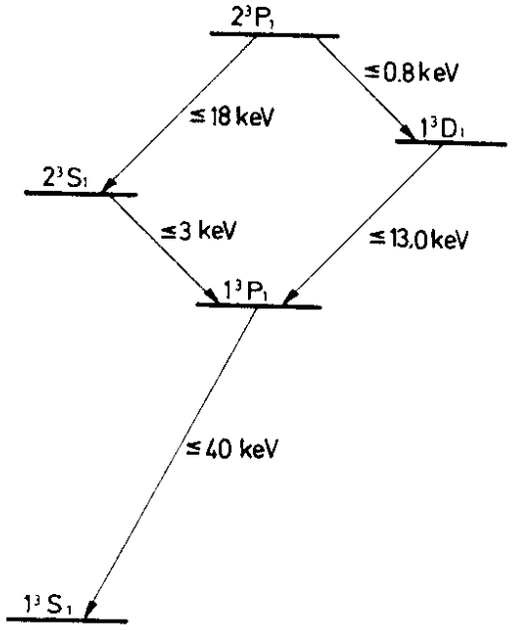

Fig. 6.3. Upper bounds for E1 transition widths in Bottonium.

The bounds in Charmonium are of more practical use at present. They are compiled in Table 6.1.

transition	TRK SR	W SR	model
$2^3S_1 \longrightarrow \gamma 1^3P_2$		< 40	36
$2^3S_1 \longrightarrow \gamma 1^3P_1$		< 56	50
$2^3S_1 \longrightarrow \gamma 1^3P_0$		< 64	58
$1^3P_2 \longrightarrow \gamma 1^3S_1$	< 490	$> 160 + 140$	460
$1^3P_1 \longrightarrow \gamma 1^3S_1$	< 370	$> 125 + 75$	350
$1^3P_0 \longrightarrow \gamma 1^3S_1$	< 180	$> 60 + 30$	170

Table 6.1: Upper and lower limits on E1 transitions from the Thomas-Reiche-Kuhn and Wigner (W) sum rules (SR). All widths in keV. The second numbers in the lower half of the W SR column arise from the second term r.h.s. of (6.28). The quark mass is taken to be $m_c = 1.6$ GeV. Also the model numbers are only sensitive to m_c.

Combining the bounds of Table 6.1 and the experimentally measured branching ratios for $P_c/\chi \to \gamma J/\psi$ one can obtain bounds for the total widths, as shown in Table 6.2.

P states	$\chi(3.41) = 0^{++}$	$P_c/\chi(3.51) = 1^{++}$	$\chi(3.55) = 2^{++}$
BR($\gamma J/\psi$), exp. [%]	3 ± 3	35 ± 7	14 ± 6
$\Gamma_{tot}(P_c/\chi)$, bounds [MeV]	3 ... 6	0.57 ... 1.05	2.15 ... 3.5

Table 6.2: Bounds on $\Gamma_{tot}(P_c/\chi)$ derived from the sum rules, Table 6.1, and the experimental BRs of $P_c/\chi \to \gamma J/\psi$. The sum rules correspond to an uncorrected E1 transition, this gives an additional theoretical uncertainty of a factor 2.

The total widths of the P_c/χ states are calculable as the sum of the radiative and the hadronic (gluon annihilation) widths. A comparison of these total widths with the bounds in Table 6.2 will be a comparison of theory with 'experiment'. This will be done in Chapter 8.

c) Magnetic Dipole Transitions

M1 decays are due to the interaction of the magnetic photon field vector $\vec{m} = \vec{k} \times \vec{\varepsilon}$ and the quark magnetic moment $\mu_Q = e \cdot e_Q / 2m_Q$. The matrix element reads

$$\langle f | \mu_Q \cdot \vec{\sigma} \cdot (\vec{k} \times \vec{\varepsilon}) | i \rangle \tag{6.31}$$

and involves the spin part of the states $|i\rangle$ and $|f\rangle$ only. We have two graphs and therefore 4 times the rate as for atomic M1 transitions [54]:

$$\Gamma(V_r \to \gamma\, PS_{r'}) = \frac{4}{3} \alpha e_Q^2 \frac{k^3}{m_Q^2} \delta_{rr'} \quad ,$$

$$\Gamma(PS_r \to \gamma\, V_{r'}) = 4 \alpha e_Q^2 \frac{k^3}{m_Q^2} \delta_{rr'} \quad . \tag{6.32}$$

An M1 transition requires $\Delta\ell = 0$ and the spatial overlap between $|i\rangle$ and $|f\rangle$ is either 1 ($r = r'$) or 0 ($r \neq r'$, forbidden M1) in this approximation.

Relativistic corrections of course modify the rate (6.32) and lead to small transitions also between orthogonal (r = r') states. In allowed transitions (r = r') the spatial overlap of one should not be changed much by relativistic corrections (but compare section 7).

d) Problems with M1 in Charmonium

In Fig. 6.4 possible candidates for the pseudoscalar partners of J/ψ and ψ' and the corresponding M1 transitions are shown. If the second χ is not at 3.59 GeV but at 3.18 GeV (second experimental solution) it can hardly be explained as a pseudoscalar. In the figure the calculated M1 widths are shown.

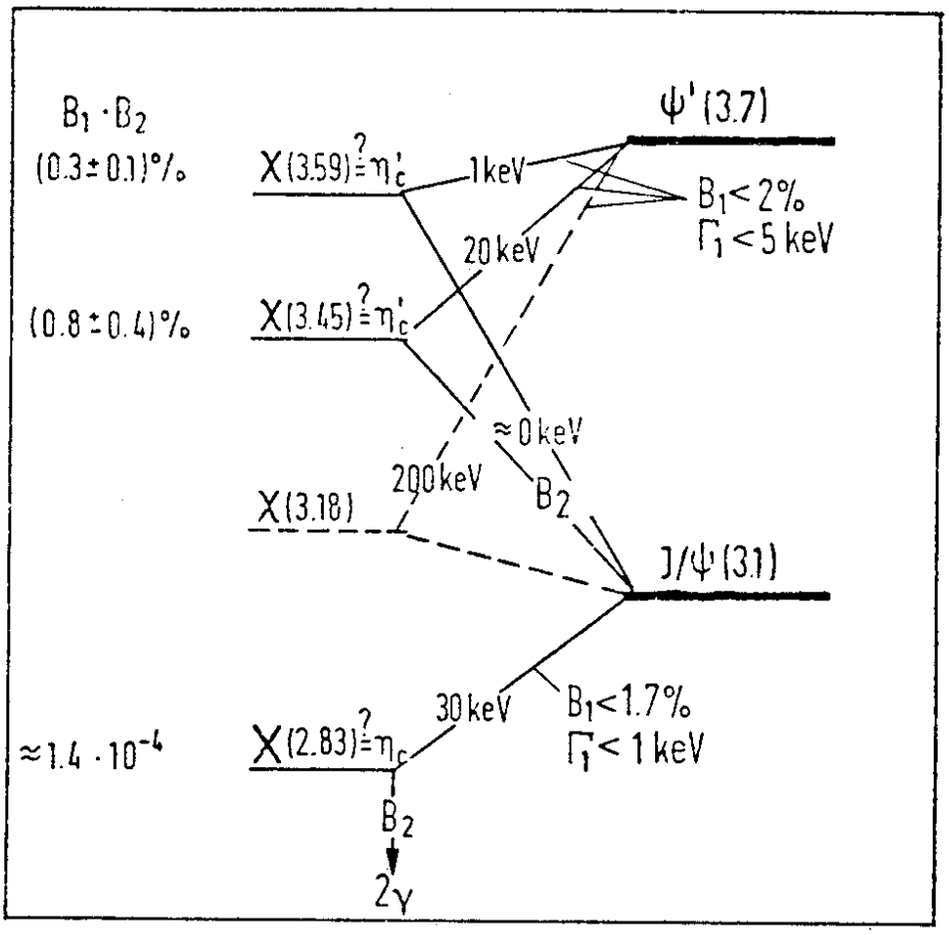

Fig. 6.4: M1 transitions in Charmonium. Theoretical widths, eq. (6.32) are indicated at the transition lines. $B_1(\Gamma_1)$ and $B_1 \cdot B_2$ are from experiment, Ref. 1), 60).

They have at first to be contrasted with the experimental bounds on these transitions as indicated. Together with the experimental product of branching ratios these bounds allow to derive lower limits on the decay branching fractions

of these states, as shown in Table 6.3. There is no way of assigning one of the experimental states to a pseudoscalar without coming into conflict with a) absolute M1 widths, b) branching fractions for the decay of this state. In the next Chapter we shall discuss alternatives which have been proposed in the literature.

State	$\chi(3.59)$	$\chi(3.45)$	$\chi(2.83)$
$B_1 \cdot B_2$ (Exp.) [%]	0.3 ± 0.1	0.8 ± 0.4	0.014 ± 0.004
B_1 (Exp.) [%]	< 2	< 2	< 1.7
B_1 (Theory) [%]	$\simeq 0.5$	$\simeq 9$	$\simeq 45$
B_2 (Exp.) [%]	> 10	> 20	> 0.7
B_2 (Theory) [%]	< 1	< 1	≈ 0.1

Table 6.3: Experimental upper bounds on B_1 and lower bounds on B_2 via $B_1 \cdot B_2$, and comparison with theory. The kind of transition for B_1, B_2 is indicated in Fig. 6.4. The theoretical numbers arise from allowed and "forbidden" M1 transitions and the ratio of 2γ versus 2 gluon annihilation. For the latter see Chapter 8. The forbidden M1 transition should lead to a B_2 not bigger than a few 10 keV/a few MeV $\approx 10^{-2}$.

e) Scaling of E1 and M1 transitions

For E1 transitions the scaling behaviour is most easily obtained from the sum rules:

$$\Gamma \sim \frac{k^3}{k^{(0)}} \frac{1}{m_Q} \approx \frac{k^2}{m_Q} \tag{6.33}$$

M1 transitions, on the other hand, scale like

$$\Gamma \sim \mu_Q^2 k^3 \sim \frac{k^3}{m_Q^2} \tag{6.34}$$

The ratio M1/E1 scales like k/m_Q. A comparison of related radiative transitions in Charmonium, Bottonium and eventually Toponium can thus help to distinguish E1 from M1 transitions.

7. The X(2.83), χ(3.45) and χ(3.59/3.18) Puzzles

In Chapter 4 we learned that the mass splittings J/ψ - X(2.83) and ψ'- χ are a factor three larger than naively expected. But the really important point which disfavours the interpretation of X and any χ as the pseudoscalar partners of J/ψ and ψ' is the following: The radiative M1 transitions, which should be allowed, are by factors 5 to 30 smaller than expected. The branching fraction of the forbidden transition $\chi(3.45) \rightarrow \gamma J/\psi$ is at least a factor 20 larger than estimated. Similarly the $B(X(2.83) \rightarrow 2\gamma)$ is about one order of magnitude larger than predicted in Charmonium. These numbers were shown in Fig. 6.4 and Table 6.3. The discrepancies with the M1 transitions are most puzzling, because related estimates in the 'old' meson spectroscopy work within a factor 2 or better. We just like to recall the famous $\omega \rightarrow \gamma\pi^0$ transition [61].

The pleasant solution would be to find the true pseudoscalars much closer to J/ψ and ψ' respectively. Experimentally this is not ruled out. Then, however, the X and χ states are either not real or at least no simple $Q\bar{Q}$ states.

At the 1977 Hamburg Conference Gottfried [51] has enumerated possible explanations for the X and χ(3.45) states. We are going to repeat them and add some new speculations (the following also applies to χ(3.59/3.18)).

There is the suggestion of 4 quark states $c\bar{c}q\bar{q}$ with all quarks in the same orbital state. De Rújula and Jaffe [62] estimate a $j^P = 0^+$ level at 3.6 GeV. This model suffers from a disease: The hadronic width must be large because it can decay Zweig allowed into $\chi\pi$ or $\chi\eta$ if it has I = 1 or 0.

Lipkin [63] has a similar idea. He argues that estimates of masses of 4 quark states are unreliable, but the level ordering is to be taken seriously. He further assigns the states $\delta(970)\,[I = 1, j^P = 0^+]$ and $S^*(993)\,[I = 0,\ j^P = 0^+]$ to the configurations $(s\bar{s}q\bar{q}')$, both below the $\phi(s\bar{s})$. By analogy one would expect $c\bar{c}q\bar{q}'$ to lie below J/ψ. The states would be Zweig stable and possibly narrow enough to be assigned to an I = 0,1 doublet X(2.83). It is to be noted that the transitions $J/\psi \rightarrow X\gamma$, $\psi' \rightarrow \chi\gamma$ are now of E1 type and $\psi' \rightarrow X\gamma$ has lot of phase space and, maybe, a sizeable dipole matrix element! To test the idea, one should search for the transitions $\psi' \rightarrow X\rho$ and $\psi' \rightarrow \gamma\chi(3.51) \rightarrow \gamma X\pi$. Their observation would show that X is not a $c\bar{c}$ state. The χ(3.45) could be fitted into this

scheme as a 0^+ $c\bar{c}s\bar{s}$ state. In a recent paper Eilam, Margolis and Rudaz [64] discuss the X(2.88) production in $\pi^- p \to \gamma\gamma n$ at 40 GeV/c [65].

Another explanation for $\chi(3.45)$ was given by the authors [66]: In the Bethe Salpeter framework with strong binding there are excitations also in the relative time coordinate, which have no analogue in the nonrelativistic Schrödinger equation. The first extra C = + state is a 'time like' P wave with $j^{PC} = 0^{++}$ or 1^{++}, depending on the Dirac structure of the model. The γ-ray transitions become of E1 type. However, this model offers no explanation for the X(2.83), besides being the 0^{-+} ground state.

Harari proposed that the $\chi(3.45)$ is the $c\bar{c}$ state $^1D_2$ [67]. However, there are problems with the magnetic transition to the J/ψ. For a detailed discussion see Ref. 55.

It could be that the $\chi(3.45)$ is a $c\bar{c}$ - gluon state [68,69]. Purely gluonic states were conjectured e.g. by Jaffe and Johnson [70]. In a recent paper, Ishikawa [71] claims a glue ball at 2.81 GeV with $j^{PC} = 0^{-+}$ which mixes with the true η_c.

We already mentioned in Chapter 4 that the contribution to the hyperfine interaction induced by the presence of instantons has been considered as a solution to the large J/ψ-X splitting. [45] However, quantitative estimates are unreliable [72] and instantons do not cure the M1 problem.

Maybe the perturbative treatment of the hyperfine interaction is grossly misleading? In a recent paper, Gromes [73] gives the following qualitative arguments: if the hyperfine splitting is essentially due to one gluon exchange, α_s must be large ($\alpha_s \simeq 0.5$). This then leads to a strongly localized and relativistic wave function of the η_c and a rather strange form of the wave function of η_c', while nothing peculiar happens to the triplet states. Overlap integrals are quite different from the naive expectation and the problems connected with radiative decays may well be solved. The hadronic width of η_c may become $\simeq$20 MeV, that of η_c' is much smaller. The branching ratio $B(\eta_c \to 2\gamma)$ remains unaffected. The naive use of the Fermi-Breit Hamiltonian for the Charmonium hyperfine splitting was already critized by Ditsas, McDougall and Moorhouse [74]. There is, however, one problem in the approach of Gromes: $\psi' \to \gamma X$ becomes an

almost allowed M1 transition. But experimentally we do not see it [1].

From all these considerations we conclude that we need additional experimental information. Maybe the first piece of new experimental information already rules out the $\chi(3.45)$: The Mark II collaboration does not find the $\chi(3.45)$ at the expected level [75].

8. Electro- and Chromomagnetic Annihilation

Quarkonium states may annihilate into photons and/or gluons. Since for non-relativistic bound states annihilation is a pointlike process, the quarks must come together to annihilate. Not only the annihilation into photons is governed by a small coupling $\alpha = 1/137$ but hopefully also that into gluons by a small α_s(small R). We can approximate the decay by the lowest order (Born-) graph [4], i.e. we can apply the 'minimal gluon scheme'. What do we mean by annihilation into gluons? Of course Quarkonium annihilates into hadrons, not gluons. However, QCD suggests that this annihilation proceeds via gluons. We can approximate the amplitude for hadronic annihilation as the product $A(Q\bar{Q} \rightarrow \text{hadrons}) = A_1(Q\bar{Q} \rightarrow \text{minimal number of gluons}) \cdot A_2$ (minimal number of gluons $\rightarrow$ hadrons). A_1 is calculable in QCD and this is what we will do. For A_2 we have to make assumptions. The simplest assumption is $A_2^2 = 1$. [4] This is an absolute upper bound. In practice A_2^2 may well be smaller. First, the gluons may be in a state with zero overlap to any known hadron system, e.g. two gluons in a spin 2 state at an invariant mass of M = 300 MeV. Second, colour bleaching effects can only make A_2^2 smaller, not larger. Third, in some regions of the three gluon phase space higher orders become very important, because a 400 MeV decay gluon cannot be discriminated against a 400 MeV confinement gluon. Realistic rates might therefore be much smaller than what we will calculate. Additionally, not only $A_2^2 = 1$ may be too optimistic, but also the calculation of A_1 in lowest order might be grossly misleading because of higher order corrections. We do not know these higher order corrections in QCD but we know the next order QED correction to the $^3S_1$ positronium decay into three photons [76]: With $\alpha = 1/3$ it would be - 100 %. But note, the more massive $Q\bar{Q}$ is the better our approximations should hold. For Charmonium they are most probably wrong. This might explain a part of the discrepancy between the α_s(annihilation), found from the calculation described above, and the α_s(spectrum). We will, however, ignore all these shortcomings and just calculate hadronic widths as gluon

annihilation widths.

We proceed as follows: first we collect well known formulae. Since in Born approximation there is no gluon selfinteraction yet, the conversion from photons to gluons is just done by redefining the charge. We will then discuss applications to Quarkonia. The results will also be relevant for the next Chapter on jets.

a) Annihilation Formulae

The vector state can decay into a lepton or quark pair (hadrons), Fig. 8.1.

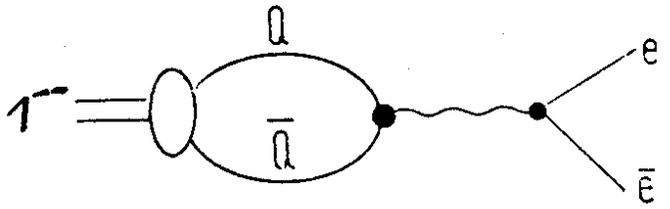

Fig. 8.1. Leptonic decay of $1^{--}(Q\bar{Q})$. The electrons may be replaced by μ's, τ's or quarks lighter than Q.

For $M_V^2 \gg 4\, m_e^2$ and including colour the formula for a $^3S_1$ state is [17]:

$$\Gamma(^3S_1 \longrightarrow e^+e^-) = \alpha^2 e_Q^2 \, |R(0)|^2 \, (M_V/2)^{-2} \tag{8.1a}$$

Here R(0) is the radial Schrödinger wave function at the origin. Quarks couple to the photon in the same way as leptons so that (8.1) is understood for each lepton or quark flavour separately: $\Gamma_{q\bar{q}} = 3e_q^2 \Gamma_{e^+e^-}$. For a $^3D_1$ state one has [55]:

$$\Gamma(^3D_1 \longrightarrow e^+e^-) = 200\, \alpha^2 e_Q^2 \, |R_D''(0)|^2 \, M_V^{-6} \tag{8.1b}$$

Numerical estimates of (8.1b) for Charmonium ($\psi''(3.77) \to e^+e^-$) only give a few eV. The experimental value for $\Gamma_{ee}(\psi''(3.77)) = 0.36$ keV [77]. So, there must be other decay mechanisms. The simplest would be an admixture of the $\psi'(3.7)$. Within the nonrelativistic bound state picture only the tensor forces, arising from one gluon exchange, mix the 2^3S_1 and 1^3D_1 wave, but numerical estimates again only give a few eV [55]. There must be another source of mixing. The Cornell group [78] proposed an S-D mixing via virtual $D\bar{D}$ states and they successfully predicted $\Gamma_{e^+e^-}$ of $\psi''(3.77)$.

The decay of 1^{--} into two photons as well as two gluons is impossible. In

the two photon case this is just the photon C parity. Also two gluons in a symmetric colour singlet state have even C. This can be seen as follows [55]: gluons can be represented by matrices in colour space, A,B,C,... There is only one way to construct a colour singlet out of two gluons A,B: Tr(AB). But Tr(AB) is even under charge conjugation. For three gluons we have two ways to construct a colour singlet, Tr(ABC) and Tr(ACB). The symmetric combination has negative C parity (D-coupling), the antisymmetric one has C = +1 (F-coupling). Therefore a 1^{--} $Q\bar{Q}$ state can decay into any number of gluons larger than two. Remember that for electromagnetic decays only an odd number of photons is allowed: photons are C eigenstates.

In lowest order the 1^{--} can decay into three photons as well as three gluons or one photon plus two gluons. The three photon decay of $^3S_1$, Fig. 8.2. has been originally calculated by Ore and Powell [79] (here including the statistical colour factor):

$$\left| \begin{array}{l} \Gamma(^3S_1 \to 3\gamma) \quad [79] \\ \Gamma(^3S_1 \to 3g) \quad [4] \\ \Gamma(^3S_1 \to \gamma 2g) \quad [80] \end{array} \right| = \left| \begin{array}{l} \frac{4}{3}\alpha^3 e_Q^6 \\ \frac{10}{81}\alpha_s^3 \\ \frac{8}{9}\alpha e_Q^2 \alpha_s^2 \end{array} \right| \cdot \frac{\pi^2 - 9}{\pi} \frac{|R(0)|^2}{m_Q^2} \qquad (8.2)$$

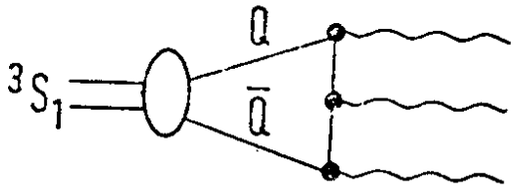

Fig. 8.2.: 3γ decay of $^3S_1(Q\bar{Q})$. When the photons are replaced by gluons, this denotes the "direct" hadronic decay.

The conversion factor from the three photon to the three gluon decay is [55]

$$\Gamma_{3g}/\Gamma_{3\gamma} = \frac{\alpha_s^3}{\alpha^3 e_Q^6} \cdot \frac{1}{9} \sum_{a,b,c} \left| Tr\left(\frac{\lambda^a}{2}\frac{\lambda^b}{2}\frac{\lambda^c}{2}\right)_{sym.}\right|^2 \qquad (8.3)$$

and has the following origin: $\alpha_s^3/\alpha^3 e_Q^6$ just converts the charges together with $|Tr(\frac{\lambda^a}{2}\frac{\lambda^b}{2}\frac{\lambda^c}{2})_{sym}|^2$. The $\Sigma_{a,b,c}$ counts the number of coloured graphs in the 3 g case, while the 3^{-2} counts the number of coloured graphs in the 3γ case.

The pseudoscalar $^1S_0$ ground state can decay into two photons or two gluons in lowest order, Fig. 8.3.

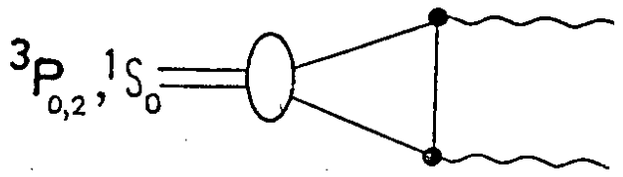

Fig. 8.3.: 2γ decay of $Q\bar{Q}$. For the hadronic decay the photons are replaced by gluons.

The two photon decay was first calculated by Pomeranchuk [81]. Including colour one has

$$\left| \frac{\Gamma(^1S_0 \longrightarrow 2\gamma)}{\Gamma(^1S_0 \longrightarrow 2g)} \right|^{\begin{matrix}81)\\4)\end{matrix}} = \left| \frac{3\alpha^2 e_Q^4}{\frac{2}{3}\alpha_s^2} \right| \frac{|R(0)|^2}{m_Q^2} \tag{8.4}$$

with the conversion factor

$$\Gamma_{2g} / \Gamma_{2\gamma} = \frac{\alpha_s^2}{\alpha^2 e_Q^4} \frac{1}{9} \sum_{a,b} \left| Tr\left(\frac{\lambda^a}{2} \frac{\lambda^b}{2}\right) \right|^2 . \tag{8.5}$$

We do not discuss the decay into more photons or gluons. Assuming that the 2 g decay is the basic process for the dominant hadronic decay of the pseudoscalar, Eq. (8.5) yielded the branching fraction for the 2γ decay (Table 6.3.)

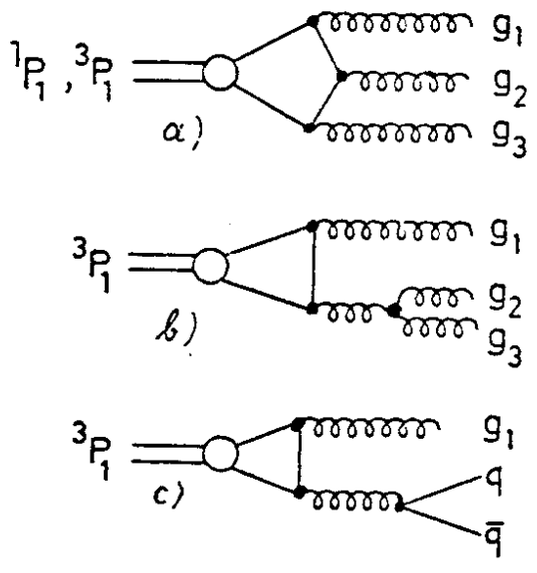

Fig. 8.4.: The gluonic decay diagrams of spin 1 P waves.

We now turn to P wave annihilation, Figs. 8.3 and 8.4. In a P wave the wave function at the origin is zero. That means that the quarks do not like to come together to annihilate. The P waves, however, can annihilate when the two quarks come near each other and simultaneously have a relative velocity $\neq 0$. This is a higher order process in $\beta^2 = (v/c)^2$. It is governed by the spatial derivative of the wave function. The annihilation widths of P waves will be smaller than that of the $^1S_0$ wave! The widths of the spin 0 and spin 2 P waves of Positronium have first been calculated by Alekseev [82]. The same calculation for Charmonium has been done by Barbieri, Gatto and Kögerler [83]. They yield

$$\left| \frac{\Gamma(^3P_0 \to 2g)}{\Gamma(^3P_2 \to 2g)} \right| = \left| \frac{6\alpha_s^2}{\frac{8}{5}\alpha_s^2} \right| \frac{|R_P'(0)|^2}{m_Q^4} \tag{8.6}$$

The 2γ width of $^3P_{0,2}$ can be obtained from (8.6) by the conversion factor (8.5). It is interesting to note that the two gluons in the $^3P_2$ decay come out with opposite helicities (➡), $J_z = \pm 2$ [84]

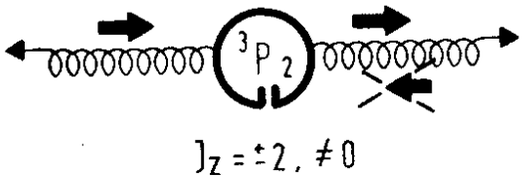

(8.7)

whereas in the $^3P_0$ decay both gluons necessarily have the same helicity. The decays of the $j = 1$ P waves are more complicated. A spin 1 state cannot decay into two massless vector bosons, either photons or gluons in a colour singlet [85]. We therefore have to consider the next order (in α_s) diagrams, which for gluon annihilation are shown in Fig. 8.4. They bring up another complication. We now have a three body phase space and have to integrate over all possible energies of, say, gluon 1. Gluon 1 is allowed to be soft. It further is allowed to carry away the angular momentum of the P wave. So it has all characteristics of a bremsstrahlungs gluon. The same is true for photon annihilation, except that in this case diagram b) of Fig. 8.4 is absent. A bremsstrahlungs gluon or photon in the annihilation of a <u>free</u> $Q\bar{Q}$ pair with $\ell = 1$ leads to the typical bremsstrahlungs singularity. The cross section factorizes into the bremsstrahlungs part and the annihilation of an $\ell = 0$ $Q\bar{Q}$ pair into two photons or gluons. For a bound state, however, the annihilation amplitude cannot be singular, because the quarks are <u>not</u> on shell. Their virtuality is of the order of the bound state dimensions. For a bound state annihilation we therefore may cut the amplitude at momenta of the soft (bremsstrahlungs) photon or gluon which correspond to the bound state radius. In diagram language, the singularity will be cancelled by higher order graphs like vertex corrections. For QED this procedure is well defined [86]. We hope that it will work parallel for QCD. As a cutoff momentum for QCD annihilation we take the typical momentum for a soft "confinement" gluon, 400 MeV, since in a QCD process higher order graphs will involve such "confinement" gluons. For heavier Quarkonia one has to take the minimum of R_{Bohr}^{-1} and 400 MeV. We will express the cutoff in terms of a parameter $\Delta = 2M \cdot 400$ MeV [87], M being the

Quarkonium bound state mass. Let us first discuss the $^1P_1$ decay. This state has $j^{PC} = 1^{+-}$ and therefore only diagram a) of Fig. 8.4 can contribute, in either photon or gluon annihilation. Its decay has been calculated by Barbieri, Gatto and Remiddi [86]. They find

$$\Gamma(^1P_{1^{+-}} \to 3g) \simeq \frac{20}{9} \alpha_s^3 \frac{|R_p'(0)|^2}{m_Q^4} \log \frac{M^2}{\Delta} \tag{8.8}$$

where the log arises from the bremsstrahlungs singularity of the diagram. For the decay of the $^3P_1$ state, $j^{PC} = 1^{++}$, only diagram c) can contribute to the photon annihilation while in principle all three diagrams can contribute to the gluon annihilation. Barbieri, Gatto and Remiddi found that the singular parts of the diagrams a) and b) cancel each other. Okun and Voloshin [55] gave the general argument for this: The amplitudes a) and b) interfere, since they lead to the same final state. Since they can both be factorized into the bremsstrahlungs part times the corresponding annihilation diagram for the 2 gluon annihilation of a coloured $^3S_1$ state, also their sum can be factorized in this way. This sum, however, contains all graphs to this order for $^3S_1$ (coloured) $\to 2g$, which must be zero from unitarity arguments [55]. Neglecting the non-singular parts of amplitudes a) and b) against the singular c) means that also for the gluon annihilation the calculation of graph c) is sufficient. It gives [86,87]

$$\Gamma(^3P_{1^{++}} \to q\bar{q}g) \simeq \frac{N}{3} \frac{8\alpha_s^3}{3\pi} \frac{|R_p'(0)|^2}{m_Q^4} \left(\log \frac{M^2}{\Delta} - \frac{1}{2}\right) \tag{8.9}$$

where N is the number of light flavours q. The photon versions of (8.8) and (8.9) can be found in Ref. 55.

For completeness we note the formula for the decay of the spin 2 D wave into 2 gluons which is given by the second derivative of the wave function, this is the second order in an expansion of $\beta^2 = (v/c)^2$ and therefore even less reliable. Okun and Voloshin [55] calculated

$$\Gamma(^1D_{2^{-+}} \to 2g) = \frac{2}{3} \alpha_s^2 \frac{|R_D''(0)|^2}{m_Q^6} \tag{8.10}$$

b) Applications

The ratio of Eq.s (8.2) and (8.1a) gives

$$\frac{\Gamma(^3S_1 \longrightarrow 3g)}{\Gamma(^3S_1 \longrightarrow e^+e^-)} = \frac{10}{81}\cdot\frac{\pi^2-9}{\pi}\cdot\frac{\alpha_s^3}{\alpha^2 e_Q^2} \simeq 1440\,\frac{4}{9e_Q^2}\,\alpha_s^3 \,. \qquad (8.11)$$

If we interpret as usual the 3g annihilation as the total direct hadronic annihilation then this is a measurable quantity and we have e.g. in Charmonium

$$\frac{\Gamma(J/\psi \longrightarrow hadr)_{dir}}{\Gamma(J/\psi \longrightarrow e^+e^-)} \simeq 10 \qquad (8.12)$$

from which follows that the α_s(annihilation) is $\alpha_s \simeq 0.19$. Because of the third power of α_s in (8.11) this value is quite stable even against large corrections to the widths. But it certainly is subject to many corrections like those discussed at the beginning of this Chapter or corrections to the wave function at the origin like (4.9).

A very interesting ratio is that of Eqs. (8.6) to Eq. (8.9):

$$\begin{aligned}&\Gamma(^3P_{0^{++}} \to 2g) \;:\; \Gamma(^3P_{1^{++}} \to q\bar{q}g) \;:\; \Gamma(^3P_{2^{++}} \to 2g)\\ &= \qquad 15 \;:\; \frac{20\,N\,\alpha_s}{9\pi}\left(\log\frac{M^2}{\Delta} - \frac{1}{2}\right) \;:\; 4\end{aligned} \qquad (8.13)$$

It leads to ratios of

$$\begin{aligned}&15 : 2.1\,\alpha_s : 4 \qquad J/\psi \text{ system}\\ &15 : 5.7\,\alpha_s : 4 \text{ in the } \Upsilon \text{ system}\\ &15 : 11\,\alpha_s : 4 \qquad 30 \text{ GeV } Q\bar{Q} \text{ system}\end{aligned} \qquad (8.14)$$

We can of course calculate more than these ratios, namely the total widths of the P waves, assuming that these are given by the gluon annihilation width and radiative transition width essentially. The result is shown in Table 8.1 for Charmonium, the Υ and the $t\bar{t}$ (30 GeV) system, and compared to the quasi-experimental bounds of Table 6.2. For the calculation of Eq.s (8.6, 8, 9) we need $|\mathcal{R}'(0)|^2$. Numerical calculations give $|\mathcal{R}'_{c\bar{c}}(0)|^2 m_c^{-3} \simeq 0.024$ GeV^2, $|\mathcal{R}'_{b\bar{b}}(0)|^2 m_b^{-3} \simeq 0.012$ GeV^2 and $|\mathcal{R}'_{t\bar{t}}(0)|^2 m_t^{-3} \simeq 0.007$ GeV^2. These quantities are relatively quark mass independent. Although the widths of Table 8.1 are

	Γ_{tot} ($^3P_0$) [keV]	Γ_{tot} ($^3P_1$) [keV]	Γ_{tot} ($^3P_2$) [keV]
$c\bar{c}$ theory	4000	500	1500
$c\bar{c}$ "quasiexp."	6000 ± 6000	1000 ± 200	3200 ± 1600
$b\bar{b}$ $\alpha_s = 0.15$	350	50	150
$b\bar{b}$ $\alpha_s = 0.20$	600	80	200
$t\bar{t}$ $\alpha_s = 0.12$	85	53	60
$t\bar{t}$ $\alpha_s = 0.15$	105	56	65

Table 8.1.: Comparison of Charmonium "experiment" and theory for the P wave total widths, including the radiative transitions from Table 6.1. The "experiment" line is taken from Table 6.2, here only errors arising from BR($\gamma J/\psi$) are shown. We also give the prospects for the Υ and $t\bar{t}$ systems of 30 GeV, where the radiative transitions are included, they are $\approx$40 keV for Υ P waves (Fig. 6.3) and 50 keV for each $t\bar{t}$ P wave.

$c\bar{c}$ decay channel:	$e\bar{e}+\mu\bar{\mu}$: $\sum q\bar{q}$:	3g :	γ2g
$e_Q = 2/3$	2 : R :	$\frac{5(\pi^2-9)\alpha_s^3}{18\pi\alpha^2}$:	$\frac{8(\pi^2-9)\alpha_s^2}{9\pi\alpha}$
a) $\alpha_s = 0.19$	2 : 2.5 :	10 :	1.2
$b\bar{b}$ decay channel:	$e\bar{e}+\mu\bar{\mu}$: $\sum q\bar{q}+\tau\bar{\tau}$:	3g :	γ2g
$e_Q = -1/3$	2 : R :	$\frac{20(\pi^2-9)\alpha_s^3}{18\pi\alpha^2}$:	$\frac{8(\pi^2-9)\alpha_s^2}{9\pi\alpha}$
b) $\alpha_s = 0.15$	2 : 5 :	20 :	0.8
$\alpha_s = 0.18$	2 : 5 :	34 :	1.1
$t\bar{t}$ (30 GeV) decay channel:	$e\bar{e}+\mu\bar{\mu}$: $\sum q\bar{q}+\tau\bar{\tau}$:	3g :	γ2g
$e_Q = 2/3$	2 : R :	$\frac{5(\pi^2-9)\alpha_s^3}{18\pi\alpha^2}$:	$\frac{8(\pi^2-9)\alpha_s^2}{9\pi\alpha}$
c) $\alpha_s = 0.12$	2 : 5 :	2.5 :	0.5
$\alpha_s = 0.15$	2 : 5 :	5 :	0.8

Table 8.2.: Ratios of the ground state decay channels a) in Charmonium, b) in the Υ system, c) in a 30 GeV $t\bar{t}$ system. For Charmonium $\alpha_s = 0.19$ agrees with experiment (lowest order formulae). For Υ decays the value of α_s best compatible with experiment, $B_{\mu\bar{\mu}}$[88], seems to be 0.18 at present.

very model dependent, we conclude that the pattern of (8.14) agrees very well with the observed branching fractions of the Charmonium P waves. This is one of the successful predictions of QCD within Charmonium.

We now give ratios of widths of the $^3S_1$ decay in Table 8.2. The decay channels of the vector ground state are: i) into lepton pairs, $e\bar{e}, \mu\bar{\mu}, \tau\bar{\tau}$, ii) into $\Sigma q\bar{q}$, iii) the three gluon annihilation and iv) the annihilation into one photon and two gluons (Eq.s 8.2).

The radiative decays of J/ψ (or Υ) $^3S_1 \to \gamma +$ hadrons are very interesting because they allow to study the Zweig suppression mechanism. QCD predicts the branching ratio $\gamma 2g/3g$ to be of the order of 1/10 in Charmonium, while in the old hadron spectroscopy photon inclusive decays were usually down by a factor of 200. For Charmonium three exclusive contributions to $^3S_1 \to \gamma 2g$ have been seen so far, namely $J/\psi \to \gamma\eta, \gamma\eta', \gamma f$ with branching fractions 0.082 ± 0.01, 0.24 ± 0.07, 0.2 ± 0.07 % respectively. Billoire, Lacaze, Morel and Navelet [89] have performed a spin parity analysis of the two gluon system in $^3S_1 \to \gamma 2g$. Their result is shown in Fig. 8.5. The remarkable feature is the

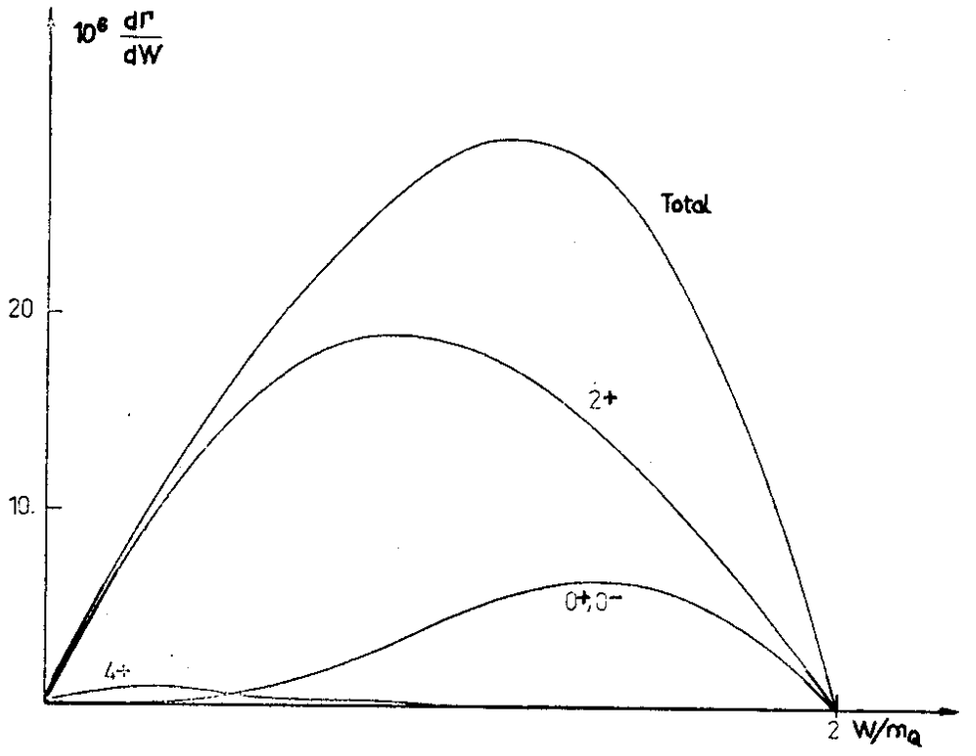

Fig. 8.5. The total hadronic mass spectrum and the contributions of $0^{\pm}$, 2^+ and 4^+ states to it. Other contributions are negligible. [89]

dominance of the 2^+ two gluon state, especially at small invariant mass W. This can be seen from the Ore-Powell matrix element:

$$\mathcal{M}_1^*(k_1,k_2,k_3;\varepsilon_1,\varepsilon_2,\varepsilon_3;K,\varepsilon) \sim \left[(k_1+k_2)\cdot k_3\,(k_2+k_3)\cdot k_1\,(k_3+k_1)\cdot k_2\right]^{-1} \times$$
$$\times \Big\{-\varepsilon_1\cdot\varepsilon_2\left[k_1\cdot k_3\,\varepsilon_3\cdot k_2\,\varepsilon^*\cdot k_1 + k_1\cdot k_3\,k_2\cdot k_3\,\varepsilon^*\cdot\varepsilon_3 + k_2\cdot k_3\,\varepsilon_3\cdot k_1\,\varepsilon^*\cdot k_2\right] +$$
$$+\varepsilon^*\cdot\varepsilon_3\left[k_3\cdot k_1\,\varepsilon_1\cdot k_2\,\varepsilon_2\cdot k_3 - k_1\cdot k_2\,\varepsilon_1\cdot k_3\,\varepsilon_2\cdot k_3 + k_2\cdot k_3\,\varepsilon_2\cdot k_1\,\varepsilon_1\cdot k_3\right] + \tag{8.15}$$
$$+ 1 \longleftrightarrow 3 \quad + \quad 2 \longleftrightarrow 3 \Big\}$$

In the limit of small gluon-gluon invariant mass $M_{1,2}^2 = (k_1 + k_2)^2 \to 0$, which for real quanta ($k_i^2 = 0$) implies $k_2 \to \lambda k_1$, $\varepsilon_2\cdot k_1 \to 0, \varepsilon_1\cdot k_2 \to 0$, it is easily checked that in this limit only the first term $\varepsilon_1\cdot\varepsilon_2\,[\ldots]$ survives [90]. From this structure follows: the helicities of the two gluons are opposite, their transverse polarizations are parallel

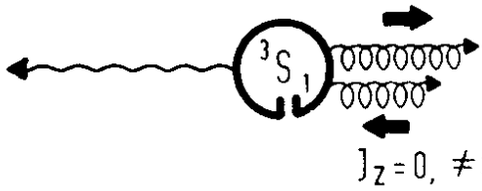

(8.16)

If we allow a finite but small two gluon mass (corresponding to a small angle between g_1 and g_2) the transformation into the two gluon rest frame yields the configuration

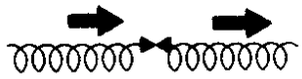

(8.17)

i.e. $J_z = \pm 2$. The gluons are now polarized in such a way that they like to couple to the $^3P_2(q\bar{q})$ state (see Eq. 8.7). Interpreting the f(1270) meson as a $^3P_2(q\bar{q})$ state the diagram

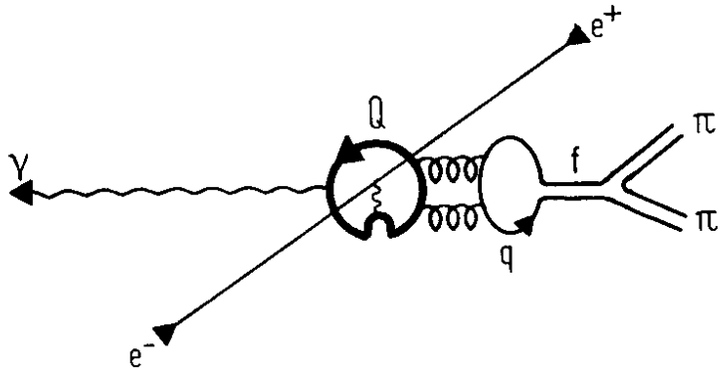

(8.18)

has been calculated [90], describing the production and decay of the f meson by three kinematically independent helicity amplitudes

$$1^{--}(1,0,-1) \longrightarrow \gamma(1) + 2^{++}(0,1,2) \equiv (A_0, A_1, A_2) \qquad (8.19)$$

which can be measured via the decay kinematics. The result of the calculation is shown in Fig. 8.6 as function of the mass ratio $M(^3P_2(q\bar{q}))/M(^3S_1(Q\bar{Q}))$. At the point $J/\psi \to \gamma f$ these amplitude ratios have been measured [91] and agree with this QCD calculation, as shown in Fig. 8.7.

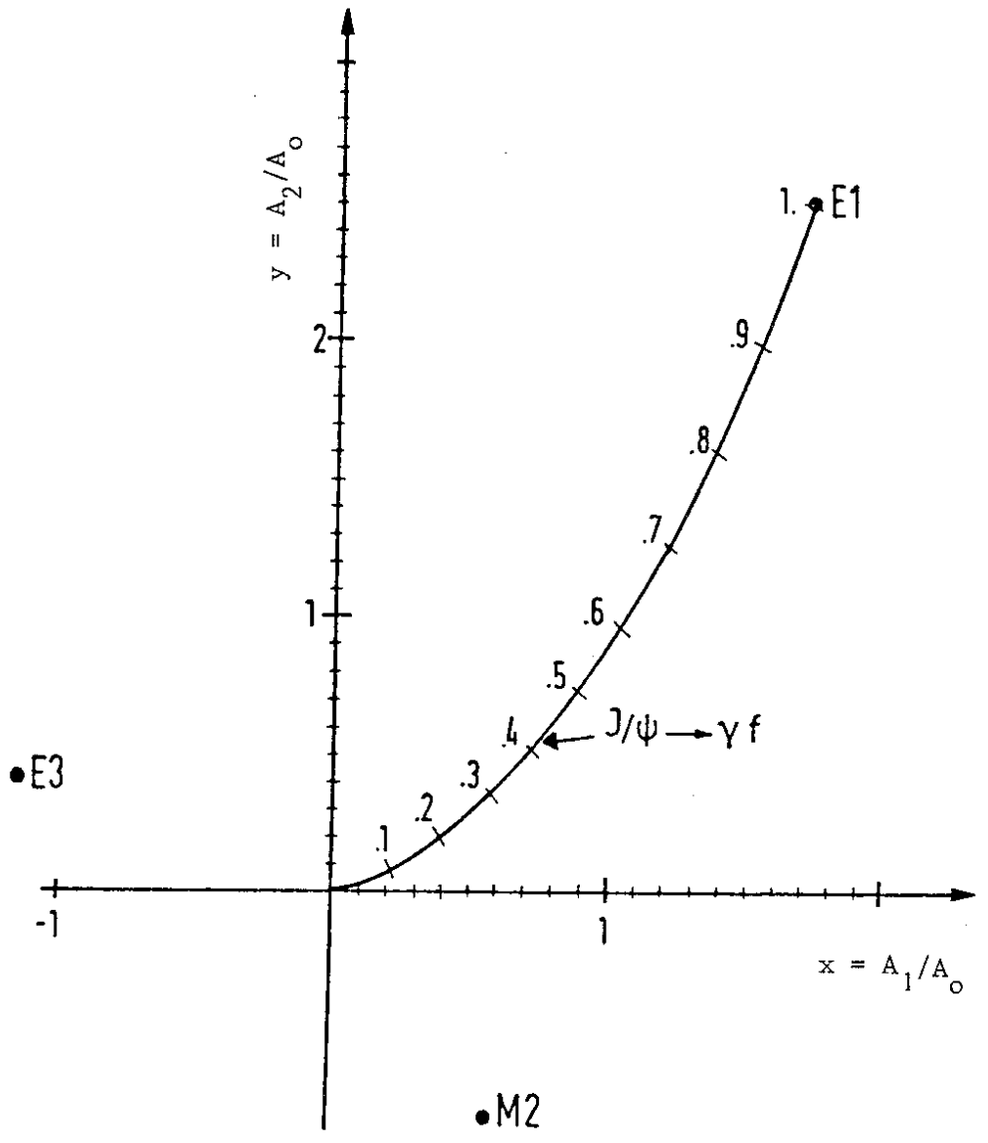

Fig. 8.6. Ratios of helicity amplitudes A_i in $^3S_1(Q\bar{Q}) \to \gamma + {}^3P_2(q\bar{q})$ as a function of $M(^3P_2)/M(Q\bar{Q})$. E1, M2, E3 denote the familiar multipole transitions, the (x,y) pair for $J/\psi \to \gamma f$ is indicated.

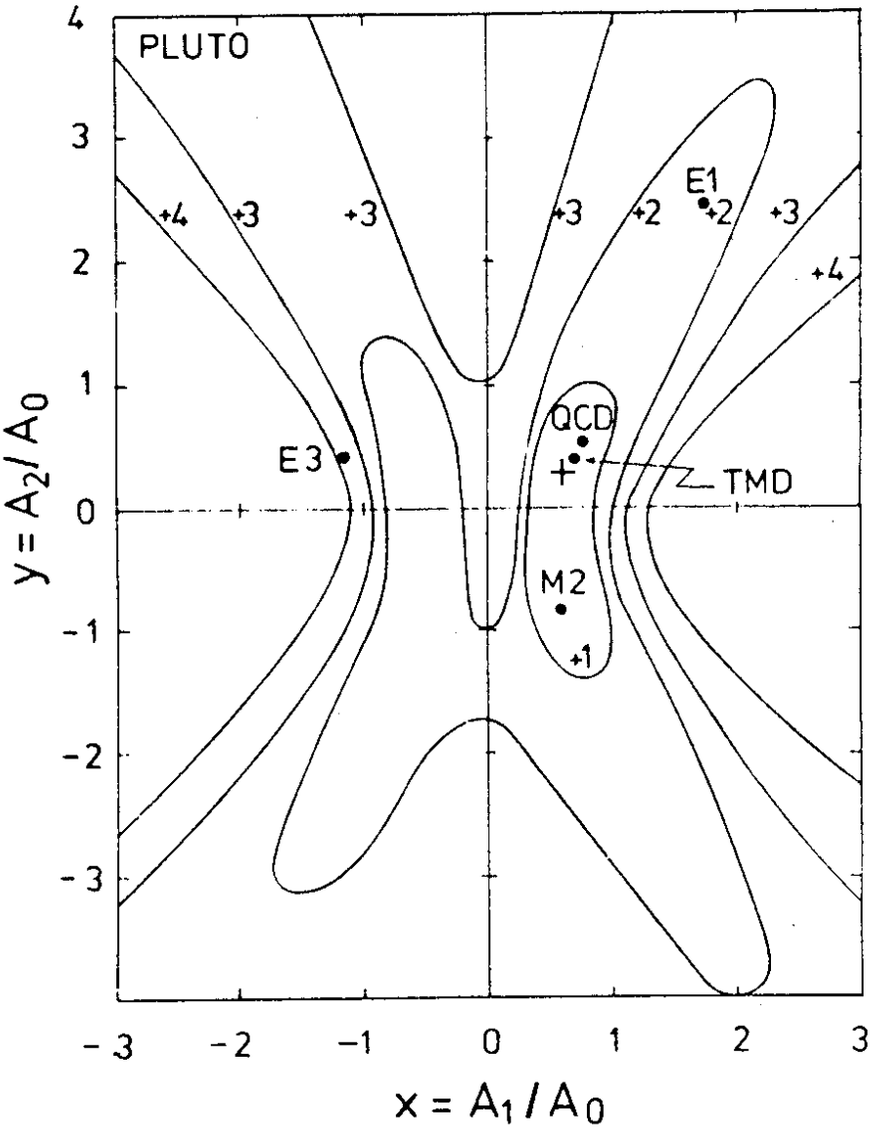

Fig. 8.7.: A measurement of the predicted (x,y) pair of Fig. 8.6 for $J/\psi \to \gamma f$ by the PLUTO collaboration. The cross is the central value of the experiment, the lines indicate standard deviations. TMD denotes the prediction of the tensor meson dominance model [92].

Billoire et al.[89] compare the $0^{\pm}$ channels where there is no 'width anomaly' at small W (see Fig. 8.5) with experiment, Fig. 8.8. The agreement with η and η' is rather satisfactory.

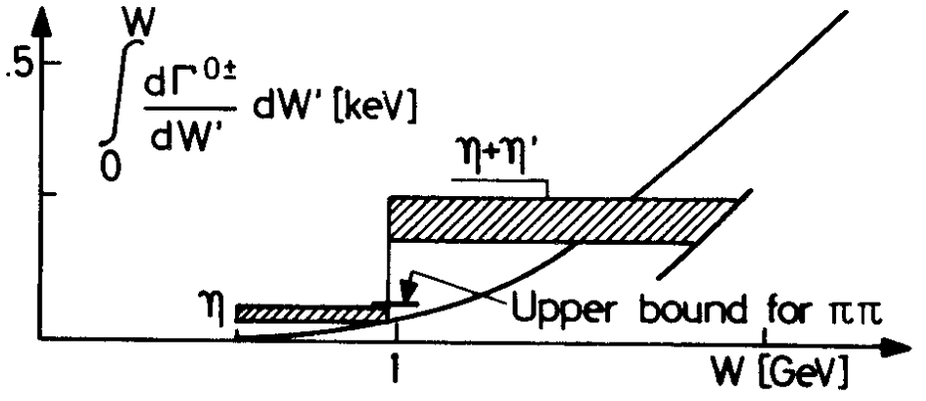

Fig. 8.8. The spectrum integrated up to W, versus W, for $0^{\pm}$ final states. The shaded area is the experimental result for $\Gamma(J/\psi \to \gamma\eta + \gamma\eta')$.

9. Jets from Quarkonia

The exploration of QCD suffers from the fact that its constituents, the quarks and gluons, cannot exist as free particles because of the confinement. Their properties cannot be investigated directly. But there is a surrogate for the observation of the free constituents, that are the jets. Experimentally jets are observed not only in deep inelastic hadron-hadron and lepton-hadron scattering but especially in e^+e^- annihilation, once the c.m. energy of 5 GeV is exceeded. The angular distribution of these jets is completely consistent with the production of two spin 1/2 (almost) massless particles [93,94], the quarks, via photon vacuum polarisation. The fragmentation of quarks or gluons into hadrons is imagined as a nonperturbative confinement effect, which conserves the original directed momenta.

At present there is no way of calculating this process, but there exists a very suggestive picture: Inside a small space region with $\simeq 1/2$ fm radius colour can exist and within this region the $q\bar{q}$ pair (or gluon) production is a short distance effect (see Fig. 9.1). When hard coloured quanta (quarks or gluons) with momenta p_i reach the confinement sphere they must fragment into white hadrons since colour fields cannot exist outside this sphere. The coloured quanta break up into hadrons with a finite perpendicular momentum $p_\perp$. This breaking up is energetically much favoured over a further existence as coloured quanta. When the perpendicular momenta are small compared to the longitudinal hadron momenta, which add up to the momentum of the original quantum, we see hadron jets. The confinement effects, however, are assumed to be soft, carried by long wavelength quarks and/or gluons. The wavelength corresponds to the colour bag of 1/2 fm. Therefore the jet momenta equal the original quantum momenta up to the order of 400 MeV. This picture demands the production of the original jet quanta to be a short distance effect ($\ll 1/2$ fm). This is certainly true for the (electromagnetic) quark pair production in e^+e^-. It is also true for a

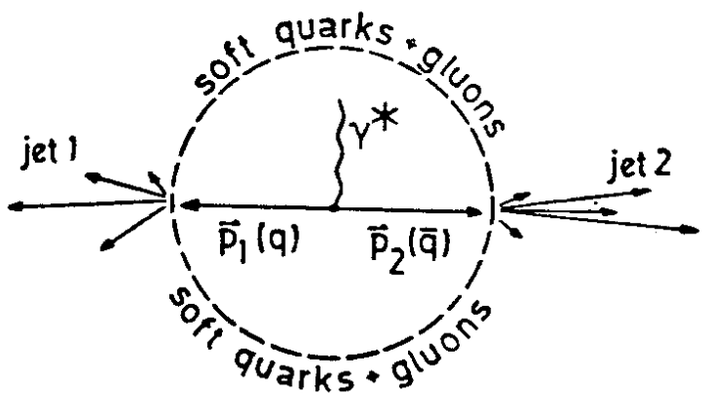

Fig. 9.1. Quark jets.

hard gluon bremsstrahlung process [95]. Resonance decays, however, are not pointlike but involve propagators (Fig. 9.2 and 9.8). Here it is not so clear, how well the jet picture will work. However, because the propagators are mass dependent the picture will work the better the higher the mass of the decaying $Q\bar{Q}$ resonance is. For a Q-mass of 5 GeV the propagator length in Fig. 9.2 is probably already short enough to apply the jet picture and for the next new flavour (higher) $Q\bar{Q}$ resonance it will definitely be so.

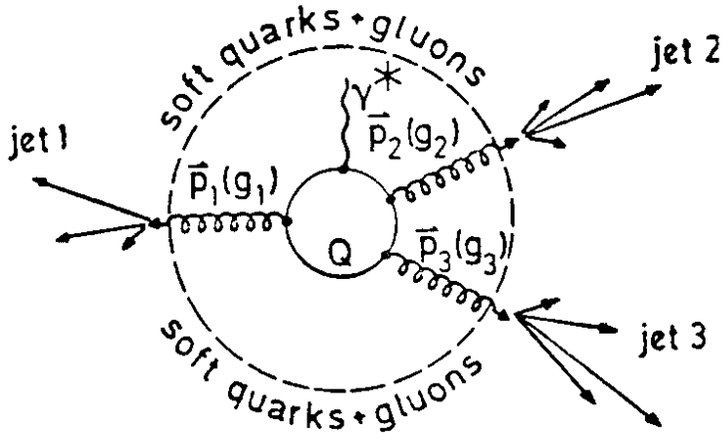

Fig. 9.2. $Q\bar{Q} \rightarrow$ 3 gluon jets.

The quark jets in e^+e^- annihilation became visible above $s = (p_1+p_2)^2 \gtrsim (5\ \text{GeV})^2$, i.e. a massless quark needs $\gtrsim$ 2.5 GeV of energy against the c.m. to be able to form a jet. The first PETRA experiments with c.m. energies up to 17 GeV show quark jets which can clearly be seen by eye and which have a fixed transverse momentum of 350 to 400 MeV [94]. This experimental evidence is - up to present energies - consistent with the nonperturbative fragmentation picture described above. What can we guess for gluon jets? For gluons the jet threshold [+)] certainly is not lower. It is equal to that of quark jets if the gluons fragment like quarks. But it can also be higher, since a gluon carries the colour indices of a quark antiquark pair and each index may fragment separately. Then the multiplicity of gluon jets may be higher and the longitudinal hadron momenta may be lower than those of quark jets. Physics will be somewhere in between. It follows that a gluon jet of a certain longitudinal momentum will have a somewhat higher multiplicity and larger opening angle than a quark jet of the same momentum. The threshold for gluon jet production will be higher than that for quark jet production.

Some possible sources of gluon jets are shown in Fig. 9.3. The pseudoscalars are omitted, they may also lead to two jets from the two decay gluons. We begin

[+)] Speaking of a jet threshold we refer to the energy of a single quark or gluon versus the center of mass of the colour bag.

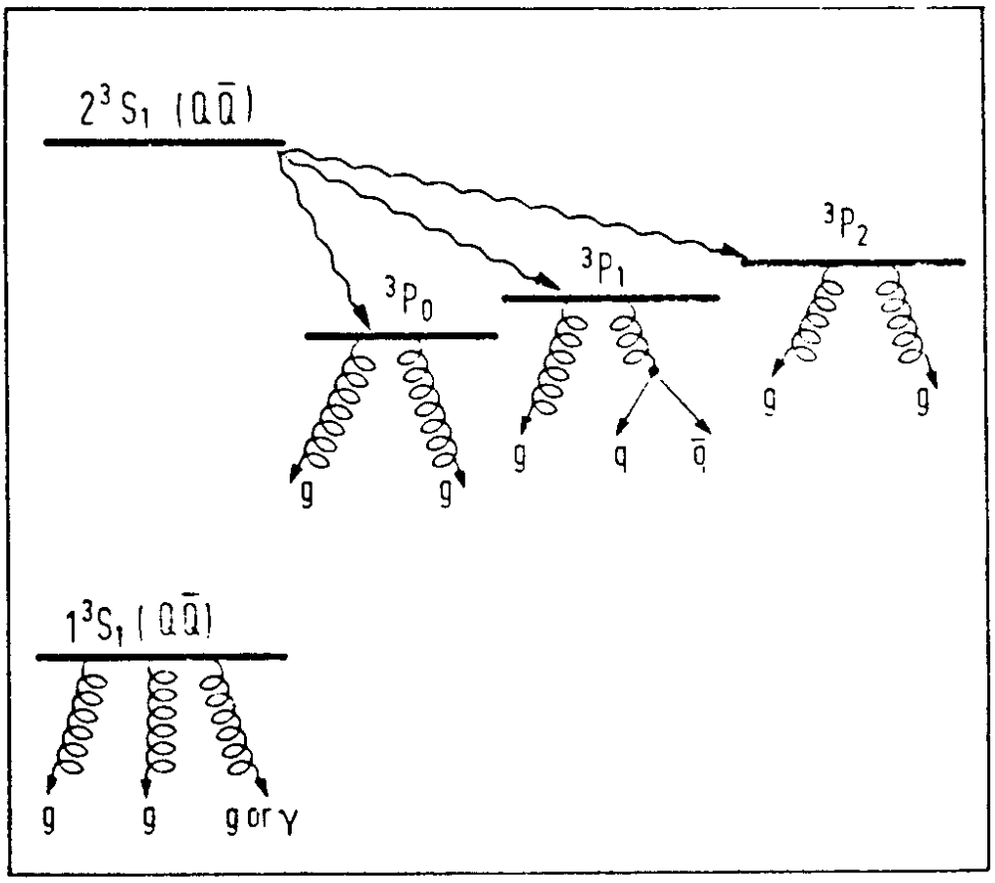

Fig. 9.3. Possible sources of gluon jets in heavy Quarkonia.

with the $^3S_1$ decay into 3 gluons. The three gluons of this decay will form a plane. The angular distribution of the normal $\hat{n}$ to this plane against the beam is

$$\frac{d\Gamma}{d\cos\theta_{\hat{n}e}} \sim 3 - \cos^2\theta_{\hat{n}e} \qquad (9.1)$$

For these decays one defines a variable T, "Thrust", [96] which in lowest order is just the scaled energy of the most energetic gluon, $T = x_1 = 2p_{g_1}/M_{Q\bar{Q}}$. The direction of g_1 defines the thrust axis. The differential rate of the 3 gluon decay together with the angular distribution of this thrust axis as calculated from the Born graph is shown in Fig. 9.4. While off resonance the coefficient of the $\cos^2$ term, α, is uniquely 1, it shows a T dependence for $Q\bar{Q}$ decays. The average $\alpha(T)$ for $Q\bar{Q} \rightarrow 3g$ is 0.39 [97]. This average can readily be compared to existing experiments [98], in contrast to the distributions of Fig. 9.4. The reason is, that experimentally we cannot measure the gluon momenta and thus the thrust as we defined it. The corresponding experimental quantity, also

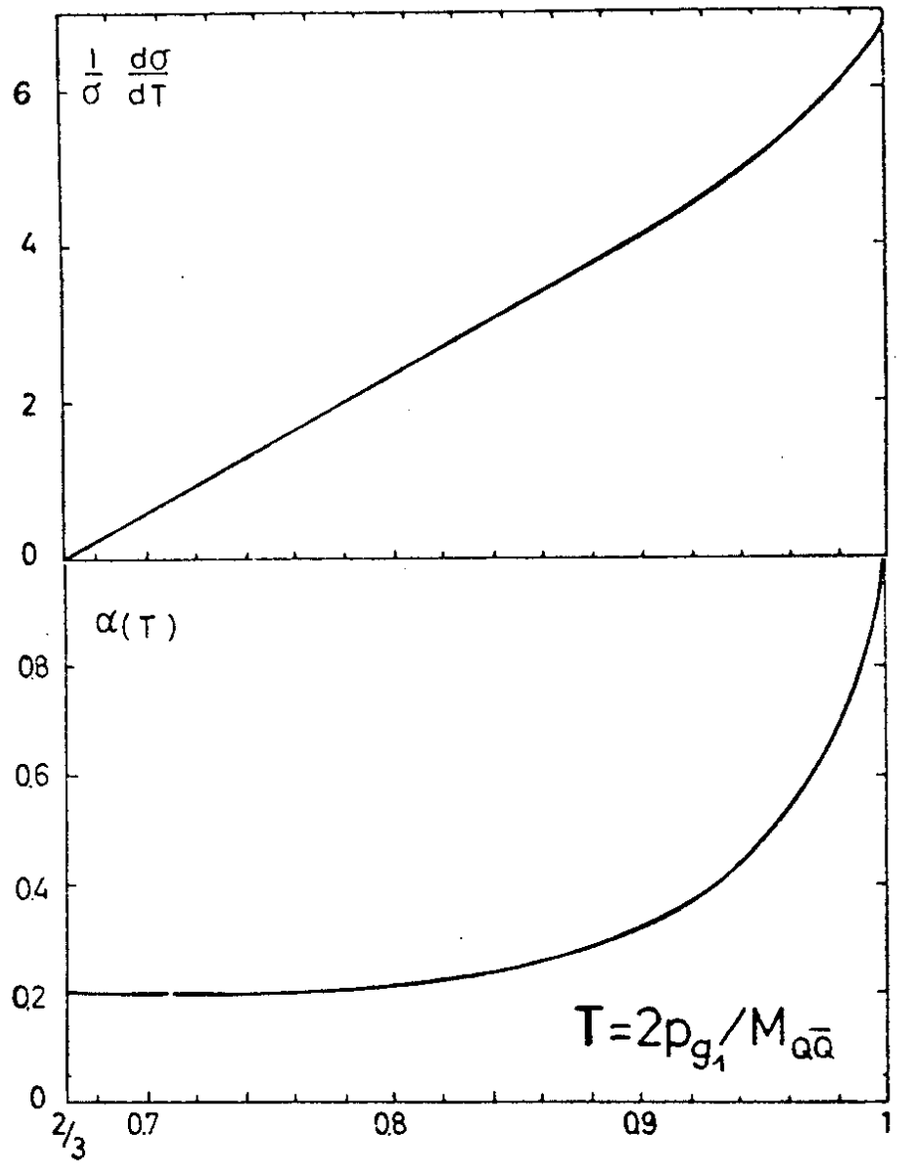

Fig. 9.4. The differential rate of $^3S_1(Q\bar{Q}) \rightarrow 3g$ and the thrust angular distribution $W \sim 1+\alpha(T)\cos^2\theta_{Te}$ as functions of T. θ_{Te} is the angle between the thrust axis and the beam.

called thrust, is $T_E = \max(\Sigma|p_\parallel|/\Sigma|p|)$ where the projection axis (the thrust axis) is chosen so that T_E is maximal. If the jet would have zero transverse momentum $x_1 = T = T_E$. But with the nonperturbative $p_\perp \neq 0$ the relation between T and T_E is only statistical. We do not know the momentum of the original jet quantum on an event by event basis. But for averages we need not know it, experimentally as well as theoretically we just sum over all events. The experimental result for the average $\alpha(T)$ in Υ decays is shown in Fig. 9.5.

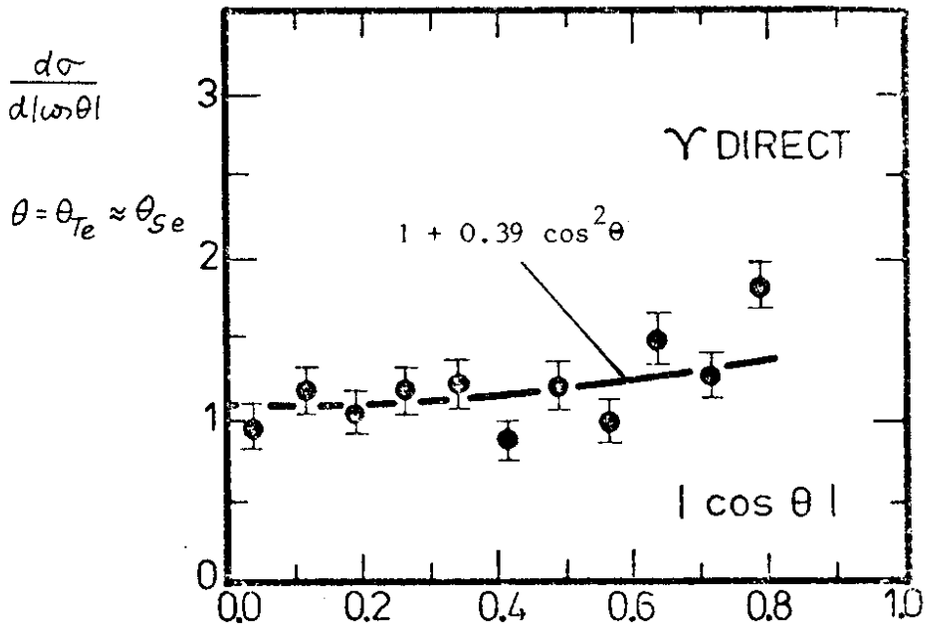

Fig. 9.5. The angular distribution of the most energetic gluon in $Q\bar{Q} \rightarrow 3g$ and the data points for $\Upsilon \rightarrow 3g$.

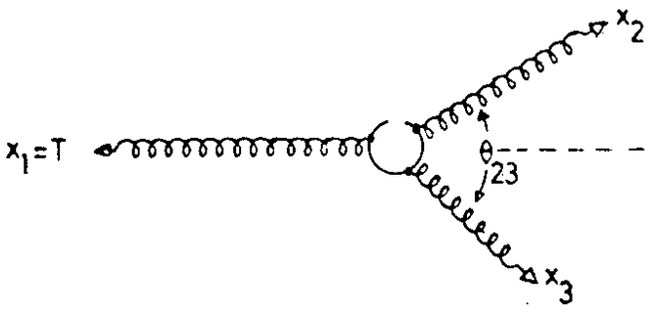

Fig. 9.6. Definition of θ_{23}.

The authors of Ref. 97) have also calculated the opening angle θ_{23} of the two gluons opposite the most energetic gluon, as defined in Fig. 9.6. Also this calculation was done in lowest order (Born graph only). Fig. 9.7 shows, if one remembers the differential rate of Fig. 9.4, that the opening angle is rather small, on the average it is only 75 degrees. If gluons fragment like quarks (which for this discussion is a conservative assumption!), one can extract the opening angle of a gluon jet from Υ decays from data on quark jets at $\sqrt{s}$ = 6 GeV: Half of the hadronic energy lies inside a cone of half angle $\delta = 30^{\circ}$ [94]. This means that an average Υ event will not show a three jet structure! Only a subsample of Υ decays with small T will show a three jet structure, e.g. for $\theta_{23} \geq 90^{\circ}$ we need to cut at $T \leq 0.85$ and are left with at most 30 % of all events. Another average to be compared to experiment is the average thrust $\langle T \rangle$ of all direct Υ decays. The perturbative value of T can be calculated, $\langle T \rangle = 0.89$. Assuming jet cones of half angle $\delta \simeq 30^{\circ}$ simple geometry allows one to calculate the value of the experimental thrust, $\langle T_E \rangle \simeq \langle T \rangle \cos\delta = 0.77$ [97]. Experimentally it is measured to be 0.76 ± 0.01 [98].

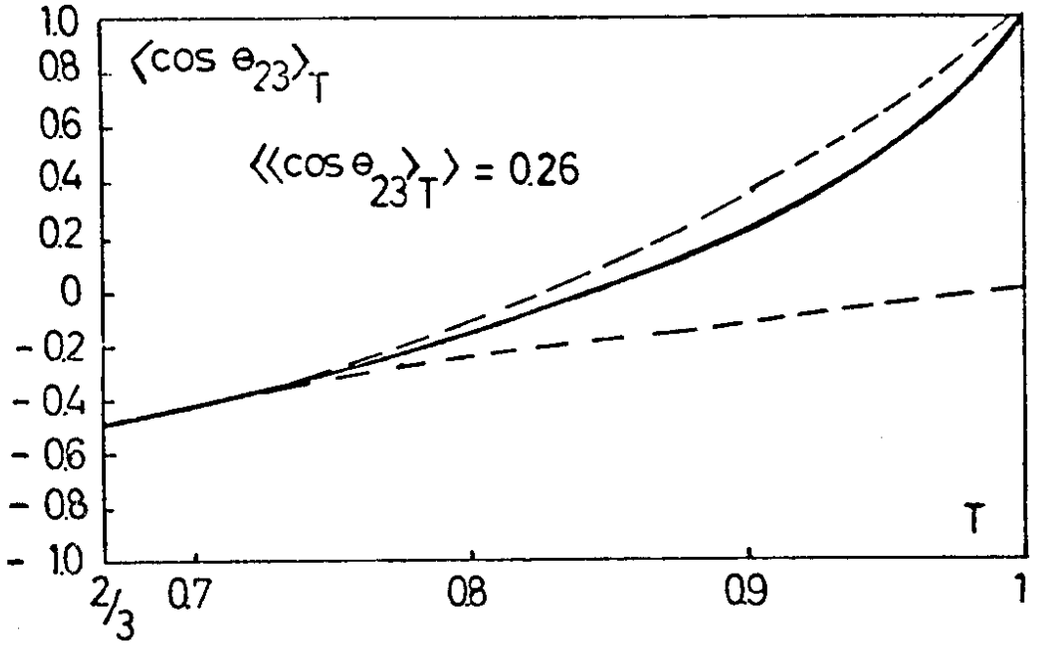

Fig. 9.7. The mean value of θ_{23}, as defined in Fig. 9.6. as a function of T. The dashed lines show the kinematic boundaries.

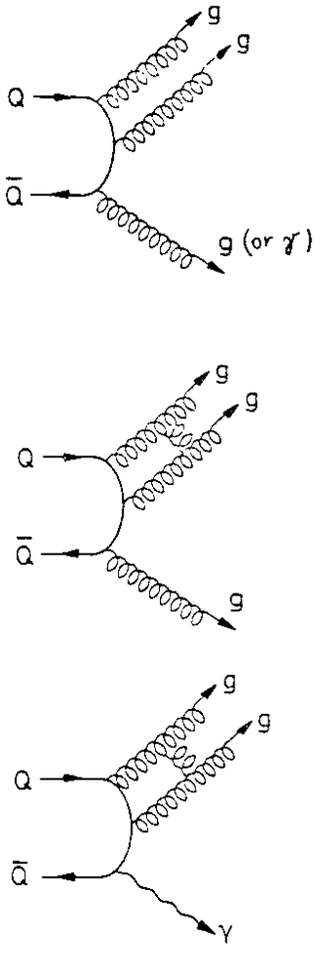

Higher order QCD calculations for Quarkonium decays into hadrons may serve as a test for the cubic (and quartic) self coupling of the gluons. De Rújula, Lautrup and Petronzio [99] have found a measure for the three gluon coupling in the next order of α_s: Interference terms like those of graphs 9.8 a plus 9.8 b allow to calculate an asymmetry of the angular distribution (9.1) when the $Q\bar{Q}$ state is produced with longitudinally polarized beams. This asymmetry is intimately related to the 3g self coupling of Fig. 9.8 b. Unfortunately cancellations occur in the calculation, so that the effect is rather small, the asymmetry is only 0.3 % in a subsample of all $Q\bar{Q}$ decays (this sample with $0.8 \lesssim T \lesssim 0.9$ contains 20 % of the events). It may therefore be more favourable to go to the next order. There we expect a change $\sim \alpha_s^2$ of the opening angle θ_{23} (Fig. 9.6) in γ2g or 3g decays of the Quarkonium ground state.

Fig. 9.8. The lowest and possible higher order (α_s) diagrams for $Q\bar{Q}$ decays.

In events with high thrust (3g) or a large photon energy (γ2g) the two gluons opposite the most energetic quantum are nearby in phase space and interact with each other according to graphs like Fig. 9.8 b and 9.8 c (there are many more graphs of course). But we see that the colour combinations of $Q\bar{Q} \rightarrow 3g$ and $Q\bar{Q} \rightarrow \gamma 2g$ are different. In the first case (hadronic decay) the two slower gluons are in a colour octet, they repel. In the second case (radiative decay) the two gluons are in a colour singlet, they attract. The effects on $\theta_{23}(T)$ of Fig. 9.7, although of order α_s^2, may well be larger than the asymmetry of order α_s discussed before, because here no cancellations should occur (we just square the amplitudes). If these speculations turn out to be true, then the decays of heavy Quarkonium ground states become a laboratory for QCD.

We now turn to jets originating from Quarkonium P wave decays. The lowest P waves can be reached from the first radially excited S wave, e.g. Υ', via an E1 transition (compare Fig. 9.3). Experimentally it will be necessary to trigger on this monochromatic photon to identify the P wave. The P state then can decay into 2 gluons in case of the $^3P_0$ and $^3P_2$ states. We will discuss the jet decay of the $^3P_1$ state later. These two gluons have a distinct energy of half the P state mass. This is the essential difference to the 3 jet decay of Quarkonium. Here we have monochromatic jets! In Υ' the jet energy is almost 5 GeV, this should be sufficient to determine the original gluon direction via the jet direction. A measurement of the gluon angular distributions becomes feasible! For the decay of the $^3P_0$ state this angular distribution is trivial: no matter, what the dynamics are, there is only one helicity amplitude which can contribute. But in the $^3P_2$ decays there are two independent helicity amplitudes for massless gluons. The QCD matrix element for the $^3P_2 \rightarrow gg$ decay reads with $q \equiv k_1 - k_2$ [13]

$$\epsilon_{\mu\nu}(\lambda)\left[4k_1\cdot k_2\,\varepsilon_1^{*\mu}\varepsilon_2^{*\nu} - \varepsilon_1^*\cdot\varepsilon_2^*\,q^\mu q^\nu + 2k_1\cdot\varepsilon_2^*\,\varepsilon_1^{*\mu}q^\nu - 2k_2\cdot\varepsilon_1^*\,\varepsilon_2^{*\mu}\cdot q^\nu\right] \quad (9.2)$$

and for on shell gluons we find the selection rule (8.7), i.e. the decay proceeds via the helicity ± 2 state. The formula for the kinematics [13] gives us, integrated, the distribution

$$W_{2g}^{2^{++}}(\theta_{\gamma j}) \sim 1 + \cos^2\theta_{\gamma j} \quad (9.3)$$

where $\theta_{\gamma j}$ is the angle between the trigger photon and one of the jets, measured in the c.m.s. of the jets (Fig. 9.9). If the $^3P_2$ would decay into two quark jets

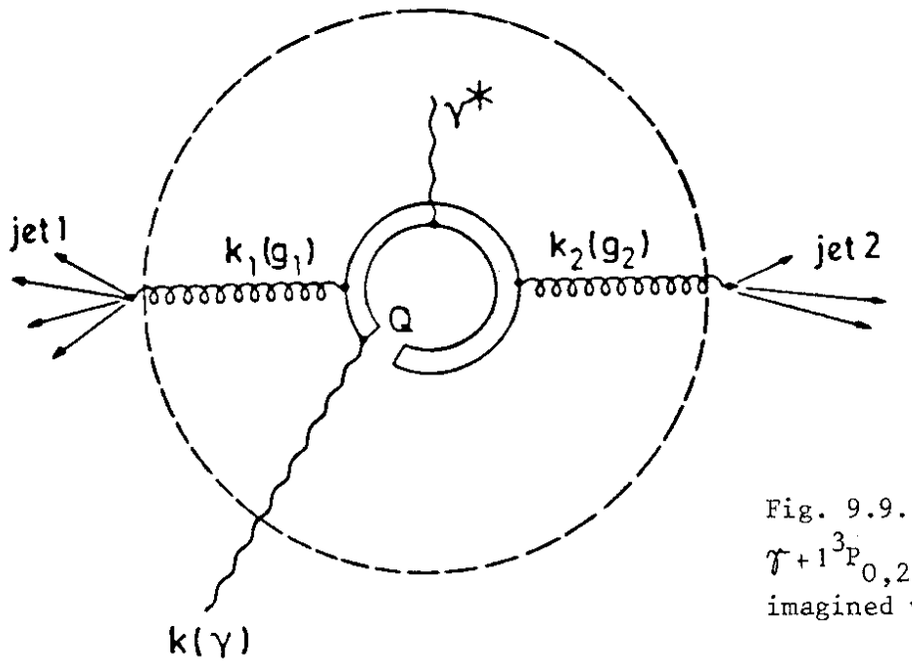

Fig. 9.9. $2^3S_1(Q\bar{Q}) \longrightarrow \gamma + 1^3P_{0,2}(Q\bar{Q}) \rightarrow \gamma +$ 2 g jets, as imagined within the colour bag.

by some arbitrary mechanism, the helicity of the two quarks can at most add up to $\lambda = \pm 1$. The kinematic formula then gives

$$W^{2^{++}}_{q\bar{q}}(\theta_{\gamma j}) \sim 1 - \frac{6 + 3A^2}{10 + 9A^2} \cos^2\theta_{\gamma j} \qquad (9.4)$$

where A gives the weight of helicities $\lambda = \pm 1$ over helicity 0. The sign difference between (9.4) and (9.3) allows a clear test of the QCD mechanism. The rate for this process will be around 5 % of all Υ' decays [13].

As we have discussed in Chapter 8) the $^3P_1$ decay proceeds via the complicated graph c) of Fig. 8.4. The decay is displayed again in Fig. 9.10. We will see two quark jets and a hadron cloud from the soft gluon from this decay. The quark jets should be easy to detect. Their angular distribution is given by

$$W^{1^{++}}_{q\bar{q}g} \sim 2 - \cos^2\theta_{\gamma e} + \cos\theta_{\gamma e}\cos\theta_{\gamma j}\cos\theta_{je} \qquad (9.5)$$

already smeared over the important kinematic regime of small gluon momentum [100]. $\theta_{\gamma j}$ is the same angle as before, $\theta_{\gamma e}$ is the angle between the trigger photon and the beam, say e^-, and θ_{je} is the angle between the same jet arm as for $\theta_{\gamma j}$ and e^-. $\theta_{\gamma e}$ is measured in the lab frame, but θ_{je} as well as $\theta_{\gamma j}$ are in the c.m.s. of the jets. As an alternative process, the decay into two massless quarks would give [100]

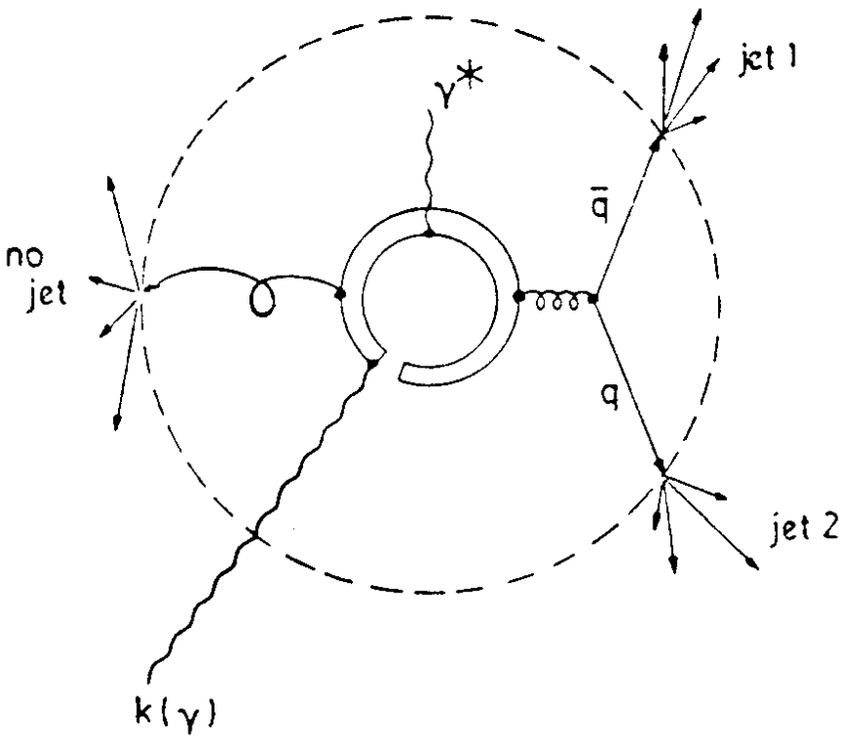

Fig. 9.10. $2^3S_1(Q\bar{Q}) \to \gamma + 1^3P_1(Q\bar{Q}) \to \gamma$ + 2 quark jets. Here a soft gluon recoils against the two quark jets.

$$W_{q\bar{q}}^{1^{++}} \sim 1 - \cos\theta_{\gamma e} \cos\theta_{\gamma j} \cos\theta_{je} \qquad (9.6)$$

Here the $\cos^2\theta_{\gamma e}$ term is missing and the term linear in the cosines has a different sign. But the most important difference between the two alternatives (9.5) and (9.6) is the recoil of the soft gluon in the $gq\bar{q}$ decay of the $^3P_1$ state. This recoil will be much larger than the recoil of the trigger photon alone which of course is always present. But with the recoil of the trigger photon alone, the 2 jets would be collinear up to a 10° deviation at most. From the recoil of the soft gluon in the decay of the $^3P_1$ state, however, the angle between the two quark jets may be as small as 110°. This is true for the Υ system. For a heavier Quarkonium the "soft" gluon may even form a third jet in a small subset of all events.

10. Conclusions and Outlook

QCD gives us hints to the static $Q\bar{Q}$ potential at short distances and allows an educated guess for long distances. The simplest potential constructed this

way, the "standard potential" $V(R) = -(4/3)\alpha_s/R + aR$ works astonishingly well in the Charmonium system. In first order perturbation theory (Breit-Fermi Hamiltonian) we are able to describe the fine structure reasonably well, while the application to the hyperfine structure might suffer from the lack of trustworthy experimental candidates. The Υ system is nonrelativistic to a much better approximation, $\beta^2 \simeq 0.08$, semirelativistic methods should give even better results here. But the attempt to describe Charmonium and Bottonium with the same static potential in the Schrödinger equation requires a modification of the "standard potential" at intermediate distances (QCD gives us no hints here). With this modification and a refinement of the short distance shape of the potential according to the distance dependence of the running coupling constant one can speculate about and predict itemsof still heavier Quarkonia yet to be discovered: Level spacings and $\Gamma_{e\bar{e}}$ will be as in Charmonium or Bottonium, but the fine and hyperfine splittings will decrease considerably. The ratio $R = \frac{\Delta M(^3P_2 - {}^3P_1)}{\Delta M(^3P_1 - {}^3P_0)}$ is interesting. It will already be close to 0.8 in Bottonium (experimentally it is 0.5 in Charmonium) and exceed 0.8 for more massive Quarkonia to approach its asymptotic value of 0.8 from above! The spectra will nevertheless look very different from Charmonium. Not only that the number of bound states below the strong decay threshold will increase like $\sqrt{m_Q}$, also the first states above threshold will be very narrow because of the large number of radial nodes in the wave function. E.g. Υ''', the first $b\bar{b}$ state above $B\bar{B}$ threshold will be very narrow, probably even below e^+e^- machine widths, thus turning out as the ideal $B\bar{B}$ factory.

The confinement part of the potential may be spin independent as suggested by lattice gauge theories. Numerical fits to Charmonium and Bottonium are consistent with a complete spin,flavour and mass independence of the long range interquark forces. Even the inverse Regge slope of the "old" mesons fits into this picture. We seem to understand parity changing photon transitions in terms of E1 radiation. This only means that we understand the "size" of Charmonium. E1 transitions of heavier Quarkonia therefore allow to test their size, too. We also seem to understand the branching fractions of P wave decays via the special QCD annihilation mechanism into two gluons. This is a short distance phenomenon. We further seem to understand radiative decays of J/ψ into γf and $\gamma\eta$ as well as $\gamma\eta'$ via simple gluon spin arguments.

Up to now we do not know any Quarkonium pseudoscalar state definitely. The

experimental candidates X(2.83), $\chi(3.45)$ and $\chi(^{3.59}_{3.18})$ can hardly be understood. Especially their M1 transitions and gluon annihilation properties should be much different from what is observed for these states.

Hadronic decays of Υ indicate the existence of gluon jets. Maybe we caught the first glimpse of the gauge bosons of the strong interactions. Our hopes for the future are that these gluon jets can finally be proven. Then Quarkonium states, S and P waves, become a laboratory for QCD. We can measure the gluon spin and verify certain QCD processes like $^3P_1 \rightarrow gq\bar{q}$. Studying the three jet decays of Quarkonium ground states we can learn about the gluon selfinteraction either by finding asymmetries or better by comparison of angular distributions of the γgg decay with the ggg decay.

Acknowledgement

We thank Professor H. Mitter and his team for the provision of an excellent atmosphere during the school, at the Stammtische and on top of the mountains. We acknowledge many discussions on the subjects of the lectures which we had with our colleagues in Hamburg.

References

1) J.J. Aubert et al., Phys. Rev. Lett. 33 (1974) 1404;
J.E. Augustin et al., Phys. Rev. Lett. 33 (1974) 1406;
G.S. Abrams et al., Phys. Rev. Lett. 33 (1974) 1453;
For reviews see:
B.H. Wiik and G. Wolf, DESY 78/23 (May 1978);
G.J. Feldman and M.L. Perl, Phys. Rep. 33C (1977) 285.

2) M. Gell-Mann, Phys. Lett. 8 (1964) 214;
G. Zweig, CERN Preprints TH 401, 412 (1964).

3) J.D. Bjorken and S.L. Glashow, Phys. Lett. 11 (1964) 255;
S.L. Glashow, J. Iliopoulos and L. Maiani, Phys. Rev. D2 (1970) 1285,
M.K. Gaillard, B.W. Lee and J.L. Rosner, Rev. Mod. Phys. 47 (1975) 277.

4) T. Appelquist and H.D. Politzer, Phys. Rev. Lett. 34 (1975) 43;
Phys. Rev. D12 (1975) 1404;
A. De Rújula and S.L. Glashow, Phys. Rev. Lett. 34 (1975) 46;
T. Appelquist et al., Phys. Rev. Lett. 34 (1975) 365;
E. Eichten et al., Phys. Rev. Lett. 34 (1975) 369.

5) S.W. Herb et al., Phys. Rev. Lett. 39 (1977) 252;
W.R. Innes et al., Phys. Rev. Lett. 39 (1977) 1240;
K. Ueno et al., Phys. Rev. Lett. 42 (1979) 486;

6) Ch. Berger et al., Phys. Lett. 76B (1978) 243;
C.W. Darden et al., Phys. Lett. 76B (1978) 246; Phys. Lett. 80B (1979) 419;
J.K. Bienlein et al., Phys. Lett. 78B (1978) 360;
C.W. Darden et al., Phys. Lett. 78B (1978) 364;
For a review see: G. Flügge, this school.

7) M. Kobayashi and K. Maskawa, Progr. Theor. Phys. 49 (1973) 652;
Y. Achiman, K. Koller and T.F. Walsh, Phys. Lett. 59B (1975) 261;
For a review see:
J. Ellis et al., Nucl. Phys. B131 (1977) 285.

8) H. Fritzsch, M. Gell-Mann and H. Leutwyler, Phys. Lett. B47 (1973) 365;
D.J. Gross and F. Wilczek, Phys. Rev. D8 (1973) 3497;
S. Weinberg, Phys. Rev. Lett. 31 (1973) 494.

9) G. 't Hooft, unpublished;
D.J. Gross and F. Wilczek, Phys. Rev. Lett. 30 (1973) 1343;
H.D. Politzer, Phys. Rev. Lett. 30 (1973) 1346.

10) For a review see: H. Joos, this school.

11) E. Eichten et al., Ref. 4.

12) J. Ellis, M.K. Gaillard and G.G. Ross, Nucl. Phys. B111 (1976) 253;
T.A. DeGrand, Y.J. Ng and S.H.H. Tye, Phys. Rev. D16 (1977) 3251;
K. Koller and T.F. Walsh, Phys. Lett. 72B (1977) 227 and 73B (1978) 504;
S.J. Brodsky, D.G. Coyne, T.A. DeGrand and R.R. Horgan, Phys. Lett. 73B (1978) 203;
H. Fritzsch and K.H. Streng, Phys. Lett. 74B (1978) 90;
K. Hagiwara, Nucl. Phys. B137 (1978) 164;
A. De Rújula et al., Nucl. Phys. B138 (1978) 387;
K. Koller and T.F. Walsh, Nucl. Phys. B140 (1978) 449;
K. Koller, H. Krasemann and T.F. Walsh, DESY 78/37 (1978).

13) M. Krammer and H. Krasemann, Phys. Lett. 73B (1978) 58;
H. Krasemann, Z. Physik C1 (1979) 189.

14) D. Robson, Nucl. Phys. B130 (1977) 328 and references therein;
P. Roy and T.F. Walsh, Phys. Lett. 78B (1978) 62.

15) V.B. Berestetski, Sov. Phys. Uspekhi 19 (1976) 934.

16) R. Barbieri et al., Nucl. Phys. B105 (1976) 125.

17) H. Pietschmann and W. Thirring, Phys. Lett. 21 (1966) 713;
R. Van Royen and V.F. Weisskopf, Nuovo Cim. 50 (1967) 617;
ibid. 51 (1967) 583.

18) R. Barbieri et al., Phys. Lett. 57B (1975) 455;
R. Karplus and A. Klein, Phys. Rev. 87 (1952) 848.

19) A. Martin, Phys. Lett. 67B (1977) 330;
H. Grosse, Phys. Lett. 68B (1977) 343.

20) E. Eichten and K. Gottfried, Phys. Lett. 66B (1977) 286.

21) C. Quigg and J.L. Rosner, Phys. Lett. 71B (1977) 153.

22) G. Bhanot and S. Rudaz, Phys. Lett. 78B (1978) 119.

23) H. Krasemann and S. Ono, DESY 79/09.

24) W. Celmaster, H. Georgi and M. Machacek, Phys. Rev. D17 (1978) 879.

25) H. Lehmann, private communication.

26) G.J. Aubrecht II and D.M. Scott, COO-1545-247.

27) See various note books.

28) G. Preparata, Ref. TH 2599-CERN.

29) W. Kummer, this school.

30) M.-A. de Crombrugghe, Phys. Lett. 80B (1979) 365.

31) H. Georgi and D.V. Nanopoulos, HUTP-78/A039.

32) H. Harari, H. Haut and J. Weyers, Phys. Lett. 78B (1978) 459.

33) S. Pakvasa and H. Sugawara, Phys. Lett. 82B (1979) 105.

34) J.D. Bjorken, SLAC-PUB 2195.

35) T.F. Walsh, DESY 78/58.

36) C. Quigg and J.L. Rosner, Phys. Lett. 72B (1978) 462.

37) J.L. Rosner, C. Quigg and H.B. Thacker, Phys. Lett. 74B (1978) 350.

38) R. Bertlmann, H. Grosse and A. Martin, Phys. Lett. 81B (1979) 59.

39) M. Krammer and P. Leal Ferreira, Rev. Brasil. Fis. 6 (1976) 7.

40) K. Ishikawa and J.J. Sakurai, UCLA-78-TEP-2; Z. Physik C1 (1979) 117.

41) M. Machacek and Y. Tomozawa, Ann. Phys. (N.Y.) 110 (1978) 407.

42) L.D. Landau and E.M. Lifshitz, Relativistic Quantum Theory (Pergamon Press, 1971); A.I. Achieser and W.B. Berestezki, Quantenelektrodynamik (Teubner, Leipzig, 1962); J. Pumplin, W. Repko and A. Sato, Phys. Rev. Lett. 35 (1975) 1538 and references therein; D. Gromes, Nucl. Phys. B131 (1977) 80.

43) For a derivation on the classical level see the text books, e.g. A. Sommerfeld, Atombau und Spektrallinien (Vieweg, Braunschweig, 1950) or J.D. Jackson, Classical Electrodynamics (J. Wiley and Sons, New York, 1962). In the framework of the Bethe Salpeter equation for Charmonium see A.B. Henriques, B.H. Kellett and R.G. Moorhouse, Phys. Lett. 64B (1976) 85.

44) See e.g.: A.I. Achieser and W.B. Berestezki, ref. 42, § 39.

45) F. Wilczek and A. Zee, Phys. Rev. Lett. 40 (1978) 83.

46) H.J. Schnitzer, Phys. Lett. 65B (1976) 239.

47) H.J. Schnitzer, Phys. Lett. 76B (1978) 461.

48) N. Isgur, Erice Lectures 1978 and references therein, Oxford Univ. Ref. 67-78; U. Ellwanger, Nucl. Phys. B139 (1978) 422.

49) H. Leutwyler and J. Stern, Phys. Lett. 73B (1978) 75.

50) K. Gottfried, Phys. Rev. Lett. 40 (1978) 598.

51) K. Gottfried, in "Proc. 1977 International Symposium on Lepton and Photon Interactions at High Energies" (DESY, F. Gutbrod ed.).

52) A. Billoire et al., preprint DPh-T/78/111.

53) J. Ellis, communication at this school.

54) See the text books, e.g. W. Heitler, The Quantum Theory of Radiation (Oxford Univ. Press, London, 1947); J.M. Blatt and V.F. Weisskopf, Theoretical Nuclear Physics (J. Wiley and Sons, New York, 1952); or S.A. Moszkowski in Beta and Gamma Ray Spectroscopy, K. Siegbahn ed. (North Holland, Amsterdam, 1955).

55) L.B. Okun and M.B. Voloshin, preprint ITEP 152 (Moscow 1976); V.A. Novikov et al., Phys. Rep. 41C (1978) 1.

56) H. Krasemann, Thesis, Hamburg 1978.

57) See e.g.: H.A. Bethe and E.E. Salpeter, Quantum Mechanics of One- and Two-Electron Atoms, Springer Verlag (Berlin, Göttingen, Heidelberg, 1957).

58) J.D. Jackson, Phys. Rev. Lett. 37 (1976) 1107.

59) L.D. Landau and E.M. Lifschitz, Relativistische Quantentheorie (Akademie-Verlag, Berlin, 1975).

60) W. Bartel et al., Phys. Lett. 79B (1978) 492.

61) C. Becchi and G. Morpurgo, Phys. Rev. 140B (1965) 687;
W. Thirring, Schladming Lectures 1965, Acta Phys. Austr. Suppl. II (1966) 205.

62) A. De Rújula and R.L. Jaffe, MIT preprint CTP 658 (August 1977).

63) H.J. Lipkin, Fermilab Conf.-77/93 THY (October 1977).

64) G. Eilam, B. Margolis and S. Rudaz, McGill Univ. preprint.

65) W.D. Apel et al., Phys. Lett. 72B (1978) 500.

66) H. Krasemann and M. Krammer, Phys. Lett. 70B (1977) 457.

67) H. Harari, Phys. Lett. 64B (1976) 469.

68) R.C. Giles and S.-H.H. Tye, Phys. Rev. D16 (1977) 1079.

69) D. Horn and J. Mandula, Phys. Rev. D17 (1978) 898.

70) R.L. Jaffe and K. Johnson, Phys. Lett. 60B (1976) 201.

71) K. Ishikawa, UCLA/78/TEP/21, (September 1978).

72) C.G. Callan et al.,Phys. Rev. D18 (1978) 4684.

73) D. Gromes, HD-THEP-79-1.

74) P. Ditsas, N.A. McDougall and R.G. Moorhouse, Nucl. Phys. B146 (1978) 191.

75) H. Taureg, talk given at DESY.

76) W.E. Caswell, G.P. Lepage and J.R. Sapirstein, Phys. Rev. Lett. 38 (1977) 488.

77) Particle Data Group, Phys. Lett. 75B (1978).

78) E. Eichten et al., Phys. Rev. Lett. 36 (1976) 500.

79) A. Ore and J.L. Powell, Phys. Rev. 75 (1949) 1696.

80) M. Chanowitz, Phys. Rev. D12 (1975) 918.

81) I. Ya. Pomeranchuk, Doklady Akademii Nauk SSSR 60 (1948) 263.

82) A.I. Alekseev, Sov. Phys. JETP 34 (1958) 826.

83) R. Barbieri, R. Gatto and R. Kögerler, Phys. Lett. 60B (1976) 183.

84) M. Krammer and H. Krasemann, Ref. 13.
The dominance of the f decay amplitude into two photons with opposite helicities has already been discussed in a different context, e.g. by:
B. Schrempp-Otto, F. Schrempp and T.F. Walsh, Phys. Lett. 36B (1971) 463;
P. Grassberger and R. Kögerler, Nucl. Phys. B106 (1976) 451.

85) C.N. Yang, Phys. Rev. 77 (1950) 242; compare also L.D. Landau and E.M. Lifshitz, Ref. 42.

86) R. Barbieri, R. Gatto and E. Remiddi, Phys. Lett. 61B (1976) 465.

87) H. Krasemann, Ref. 13.

88) C.W. Darden et al., Internal Report DESY F15-78/01 (Aug. 1978);
G. Flügge, this school.

89) A. Billoire et al., Phys. Lett. 80B (1979) 381.

90) M. Krammer, Phys. Lett. 74B (1978) 361.

91) G. Alexander et al., Phys. Lett. 76B (1978) 652.

92) See H. Genz, this school.

93) R.F. Schwitters et al., Phys. Rev. Lett. 35 (1975) 1320;
G. Hanson et al., Phys. Rev. Lett. 35 (1975) 1609;
G. Hanson, SLAC PUB 2118 (1978).

94) Ch. Berger et al., Phys. Lett. 78B (1978) 176; Phys. Lett. 81B (1979) 410;
see also G. Flügge, this school.

95) J. Ellis, M.K. Gaillard and G.G. Ross, Ref. 12.

96) S. Brandt et al., Phys. Lett. 12 (1964) 57;
E. Farhi, Phys. Rev. Lett. 39 (1977) 1587;
A. De Rújula et al., Ref. 12.

97) K. Koller, H. Krasemann and T.F. Walsh, Ref. 12.

98) Ch. Berger et al., DESY 78/71.

99) A. De Rújula, B. Lautrup and R. Petronzio, Nucl. Phys. B146 (1978) 50.

100) A. De Rújula et al., Ref. 12 and H. Krasemann, Ref. 13.